

# **Surface and Interface Research and Engineering Delft University of Technology**

**A Collection of Mini Posters**

**1997**



Editors: W.G. Sloof  
A.D. van Langeveld

Bibliotheek TU Delft



C 2322286

**8512  
124 G**

Published and distributed by:

Delft University Press  
Mekelweg 4  
2628 CD Delft  
The Netherlands  
Phone: +31.15.278 3254  
Fax: +31.15.278 1661

Cover:

*Right: Interface between  $\text{SrTiO}_3$  and  $\text{YBa}_2\text{Cu}_3\text{O}_7$  High resolution Transmission Electron Microscopy (Dr. H.W. Zandbergen).*  
*Left: Surface of an electrodeposited zinc coating on steel sheet, High resolution Scanning Electron Microscopy (Mr. C.G. Borsboom).*

CIP-DATA Koninklijke Bibliotheek, The Hague

Sloof, W.G.

Surface and Interface Research and Engineering Delft University of Technology;  
A Collection of Mini Posters 1997 / W.G. Sloof and A.D. van Langeveld - Delft:  
Delft University Press. - Ill.

ISBN 90-407-1489-4

NUGI: 841

Keywords: surfaces, thin films and interfaces.

Copyright © 1997 by Delft University Press.

No part of this book may be reproduced in any form by print, photoprint, microfilm or any other means, without written permission from the publisher: Delft University Press, Mekelweg 4, 2628 CD Delft, The Netherlands.

Printed in The Netherlands.

# Contents

<b>Preface</b>	7
----------------	---

## *Faculty of Chemical Technology and Materials Science*

<b>Applied Inorganic Chemistry</b>	9
------------------------------------	---

Chemical Vapor Deposition of Silicon Carbide Coatings on Stainless Steel <i>W.F.A. Besling, B. Meester and J. Schoonman</i>	11
--	----

In-situ Raman Spectroscopy During Laser-induced CVD of Silicon Thin Films <i>W.F.A. Besling, A. Goossens and J. Schoonman</i>	13
--	----

Morphology Control of Thin $\text{LiCoO}_2$ Films Fabricated Using Electrostatic Spray Deposition (ESD) Technique <i>Chunhua Chen, Erik. M. Kelder, Paul J.J.M. van der Put and J. Schoonman</i>	15
---	----

Effects of Additives in Electrospraying for Materials Preparation <i>C.H. Chen, E.M. Kelder and J. Schoonman</i>	17
---	----

Chemical Gas Sensor Array for the Detection of $\text{NO}_x$ and CO <i>M.H.J. Emond, R.C. van Landschoot and J. Schoonman</i>	19
--	----

Rupture of Thin Liquid Films <i>L.J. Evers</i>	21
---	----

Cuprisation of Polyetherimide by Chemical Vapour Deposition <i>M.L.H. ter Heerdt, P.J.J.M. van der Put and J. Schoonman</i>	23
--	----

The Catalytic Sensor for Detection of Natural Gas <i>L.N. van Rij, R.C. van Landschoot and J. Schoonman</i>	25
--	----

Preparation of Zirconium Dioxide Powder by Flame-Assisted Ultrasonic Spray Pyrolysis (FAUSP) <i>F.L. Yuan, C.H. Chen, E.M. Kelder and J. Schoonman</i>	27
---	----

<b>Industrial Catalysis</b>	29
-----------------------------	----

Quasi In-Situ XPS Characterisation of Different Nickel Species in $\text{NiW}/\gamma\text{-Al}_2\text{O}_3$ Hydrotreating Catalysts Upon Sulfiding <i>H. Reinhoudt, R. Mariscal, A.D. van Langeveld and J.A. Moulijn</i>	31
---	----

<b>Organic Chemistry and Catalysis</b>	33
Design of a Zeolite-based Pyroelectric Thin Film Calorimeter <i>G.J. Klap, J.C. Jansen, H. van Bekkum, M. Wübbenhorst and J. van Turnhout</i>	35
Analysing Crystal Surface Roughness by Atomic Force Microscopy <i>J.H. Koegler, E.N. Coker and J.C. Jansen</i>	37
<b>Physical Chemistry</b>	39
Adsorption and Pore Penetration of Polymers at Anodized Aluminium <i>S.G.O. de Haas</i>	41
Adsorption and Oxidation of Formaldehyde on Various Metals <i>Marnix ten Kortenaar, Gert Frens, Zvonimir Kolar and Jeroen de Goeij</i>	43
Improvement of Cohesive and Adhesive Properties of Whey Proteins <i>A.A.C.M. Rutten</i>	45
Effectivity of Detergents in Dynamic Surface Cleaning <i>A. Timmerman and G. Frens</i>	47
<b>Materials Physics</b>	49
Defects in Thin Films Produced by Ion-beam Assisted Deposition <i>Jan van der Kuur, Jacqueline van der Linden, Martin Pols, Bas Korevaar, Peter Klaver and Barend Thijsse</i>	51
<b>Physical and Chemical Materials Science</b>	53
On the Initial Oxidation of Iron: Quantification of Growth Kinetics <i>P.C.J. Graat, M.A.J. Somers and E.J. Mittemeijer</i>	55
Low- <i>T</i> Dry Oxidation on Pure Aluminium Crystal Grain Surfaces as Observed with Photoelectron and Auger Electron Spectroscopy <i>L.P.H. Jeurgens, W.G. Sloof, F.D. Tichelaar, C.G. Borsboom and E.J. Mittemeijer</i>	57
A Model for Stress in Thin Layers Induced by Misfitting Particles - An Origin for Growth Stress <i>J.-D. Kamminga, Th.H. de Keijser, R. Delhez and E.J. Mittemeijer</i>	59
Quasi In Situ Sequential Sulphidation of CoMo/Al <sub>2</sub> O <sub>3</sub> Studied Using High Resolution Electron Microscopy <i>P.J. Kooyman, J.G. Buglass, H.R. Reinhoudt, A.D. van Langeveld, H.W. Zandbergen and J.A.R. van Veen</i>	61
Growth and Annealing of Ag-Ni Layers - Stresses and Twin Densities <i>L. Veltrop, R. Delhez, Th.H. de Keijser, E.J. Mittemeijer and D. Reefman</i>	63



<b>Corrosion Technology and Electrochemistry</b>	65
Corrosion Protection of Steel in Molten Carbonates by Ceramic Coatings <i>M. Keijzer, P.J.J.M. van der Put, K. Hemmes, J.H.W. de Wit and J. Schoonman</i>	67
Electrochemical Impedance Measurements on Anodized Aluminium <i>M.B. Spoelstra, D.H. van der Weijde and J.H.W. de Wit</i>	69
<b>Heat Treatment Science and Technology</b>	71
The Effect of Inhomogeneous Nitriding on the Fatigue Strength of the Nitriding Steel En40B <i>J.J. Braam, B. Pennings and S. van der Zwaag</i>	73
Filiform Corrosion on Coated Aluminium Alloys: the Role of Microstructural Inhomogeneities in the Substrate <i>J.M.C. Mol, D.C.M. Wilms, J.H.W. de Wit and S. van der Zwaag</i>	75
<b>Advanced Materials and Casting Technology</b>	77
Metallurgical Control of Filiform Corrosion of Aluminium Rolled Products (FICARP) <i>M.H.M. Huisert, D.H. van der Weijde, J.H.W. de Wit and L. Katgerman</i>	79
<b>Faculty of Applied Physics</b>	
<b>Particle Optics</b>	81
A Parallel Detector for Auger Spectroscopy in an Electron Microscope <i>J.S. Faber, C. Smit and P. Kruit</i>	83
<b>DIMES / NanoPhysics and - Technology</b>	85
Nanoscale Structures Composed by Selective Thermal CVD and STM Stimulated Decomposition of Dimethylaluminiumhydride <i>E. Boellaard and G.C.A.M. Janssen</i>	87
Temperature Dependant Morphology Changes of CoSi <sub>2</sub> Thin Films <i>B. Ilge, G. Palasantzas, J.M.M. de Nijs and L.J. Geerligs</i>	89
High Pressure Extrusion of Aluminium for Sub-micron Vias <i>J.F. Jongste, J.P. Lokker, G.C.A.M. Janssen and S. Radelaar</i>	91
Origin of Resistance Changes due to Electromigration in Al Lines <i>A.H. Verbruggen, M.J.C. van den Homberg, L.C. Jacobs and S. Radelaar</i>	93

***Interfaculty Reactor Institute***

**Radiation Physics** 95

Production and Characterisation of Polyelectrolyte Multilayers 97  
*R. Bijlsma and A.A. van Well*

## Preface

Each year, started in 1995, we collected so called 'Mini Posters' on 'Surface and Interface Research and Engineering' at the Delft University of Technology, The Netherlands. Also this year the response to our call for Mini Posters was encouraging, as demonstrated by the contents of this booklet, which is now the third in a row. With this annual collection and publication of Mini Posters we might say that a tradition is being to establish.

The Mini Posters are mainly composed by PhD Students (so-called AIO's and OIO's). We are grateful for their contributions and enthusiasm. This compilation hopefully provides a simple and attractive overview, in particular for graduate and PhD students, who are engaged in research devoted to surfaces, thin films and interfaces.

The objective of this work would be to bring together and to realise mutual stimulation of, in particular young, scientists and at the same time to outline the research on the physics and chemistry of surfaces, thin films and interfaces at the Delft University of Technology. Major topics of interest are surface treatment and engineering, catalysis and corresponding analytical techniques.

Of course, an ultimate goal is to realise contact between the various research groups recognising that our science will flourish by exchanges of ideas and information. From this perspective, a Mini Symposium on 'Surface and Interface Research and Engineering' was held at June 20<sup>th</sup>, 1997. At this symposium, all participants had the opportunity to present their work as a full-size poster and a selected number participants were invited to give an oral presentation.

We do hope you will find reading the Mini Posters interesting and informative.

W.G. Sloof

A.D. van Langeveld.


The first part of the paper is devoted to a general discussion of the problem. It is shown that the problem is of great importance in the theory of the structure of matter. The second part is devoted to a detailed analysis of the problem. It is shown that the problem is of great importance in the theory of the structure of matter. The third part is devoted to a detailed analysis of the problem. It is shown that the problem is of great importance in the theory of the structure of matter.

The fourth part is devoted to a detailed analysis of the problem. It is shown that the problem is of great importance in the theory of the structure of matter. The fifth part is devoted to a detailed analysis of the problem. It is shown that the problem is of great importance in the theory of the structure of matter.

The sixth part is devoted to a detailed analysis of the problem. It is shown that the problem is of great importance in the theory of the structure of matter. The seventh part is devoted to a detailed analysis of the problem. It is shown that the problem is of great importance in the theory of the structure of matter.

The eighth part is devoted to a detailed analysis of the problem. It is shown that the problem is of great importance in the theory of the structure of matter.

# Applied Inorganic Chemistry

Groupleader:	Prof.dr. J. Schoonman
Addres:	Delft University of Technology
	Faculty of Chemical Technology and Materials
	Science
	Julianalaan 136
	NL 2628 BL Delft
	+31-15-278 2667
	J.Schoonman@STM.TUdelft.NL
 fax:	+31-15-278 8047



# Chemical Vapor Deposition of Silicon Carbide Coatings on Stainless Steel

*W.F.A. Besling, B. Meester, and J. Schoonman*

*Laboratory for Applied Inorganic Chemistry, Delft University of Technology*

Sponsor: AKZO Nobel

tel: +31-15-2782637

E-mail: Besling@stm.tudelft.nl

## Introduction

Silicon carbide (SiC) is an excellent candidate for structural applications due to its high resistance against corrosion and outstanding mechanical properties.

Low Pressure Chemical Vapor Deposition (LP-CVD) is one of the best techniques to deposit dense, uniform SiC. As a result LPCVD SiC is on the verge of being used in applications which require protective coatings for corrosive and abrasive environments. However, due to a large mismatch in thermal expansion coefficient between stainless steel and the SiC coating, cracks and delamination occurs resulting in bad quality films. Since most of the physical or chemical properties of SiC are strongly dependent on the processing conditions, knowledge of the deposition mechanism and surface reaction kinetics is desirable. Therefore silicon carbide deposition in a LP-CVD reactor have been studied by analyzing deposition rates as a function of temperature, reactant partial pressures and reactant ratios and the resulting properties of the deposited layers.

## Experimental

Tetramethyl silane (TMS) is used as a single source precursor. The depositions are carried out on duplex and 316 stainless steel substrates. Temperature is varied from 800°C to 1000°C. Reactor pressure is around 1.0 torr.

## Results

The deposition rate is exponentially dependent on the deposition temperature. At 900°C growth rates are obtained of 0.5  $\mu\text{m/h}$  in a reaction controlled regime. At

temperatures above 1000 °C the layers become rough indicating a diffusion controlled regime. EPMA showed a carbon rich SiC phase with, in some cases, some oxygen contamination (up to 2 at.%). Upon increasing the temperature from 900°C to 1000°C, the free carbon content decreases from 23 at.% to 18 at. %. XPS analysis indicated Si-C bonding and the presence of free carbon. Cubic SiC is deposited above 1000°C while an amorphous phase is formed at lower temperatures.

Radial oriented V-shaped cracks are observed on duplex steel indicating large thermal stresses. Corrosion experiments in concentrated  $\text{H}_3\text{PO}_4$  revealed that SiC is not attacked, while the duplex steel is corroded very rapidly where bare steel was exposed under some cracks.

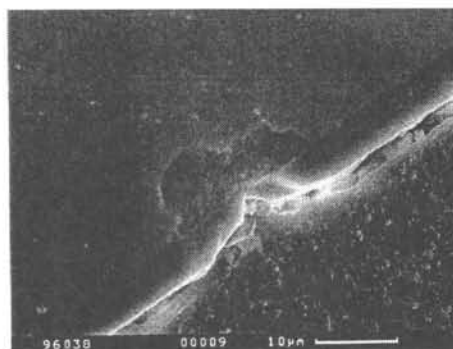
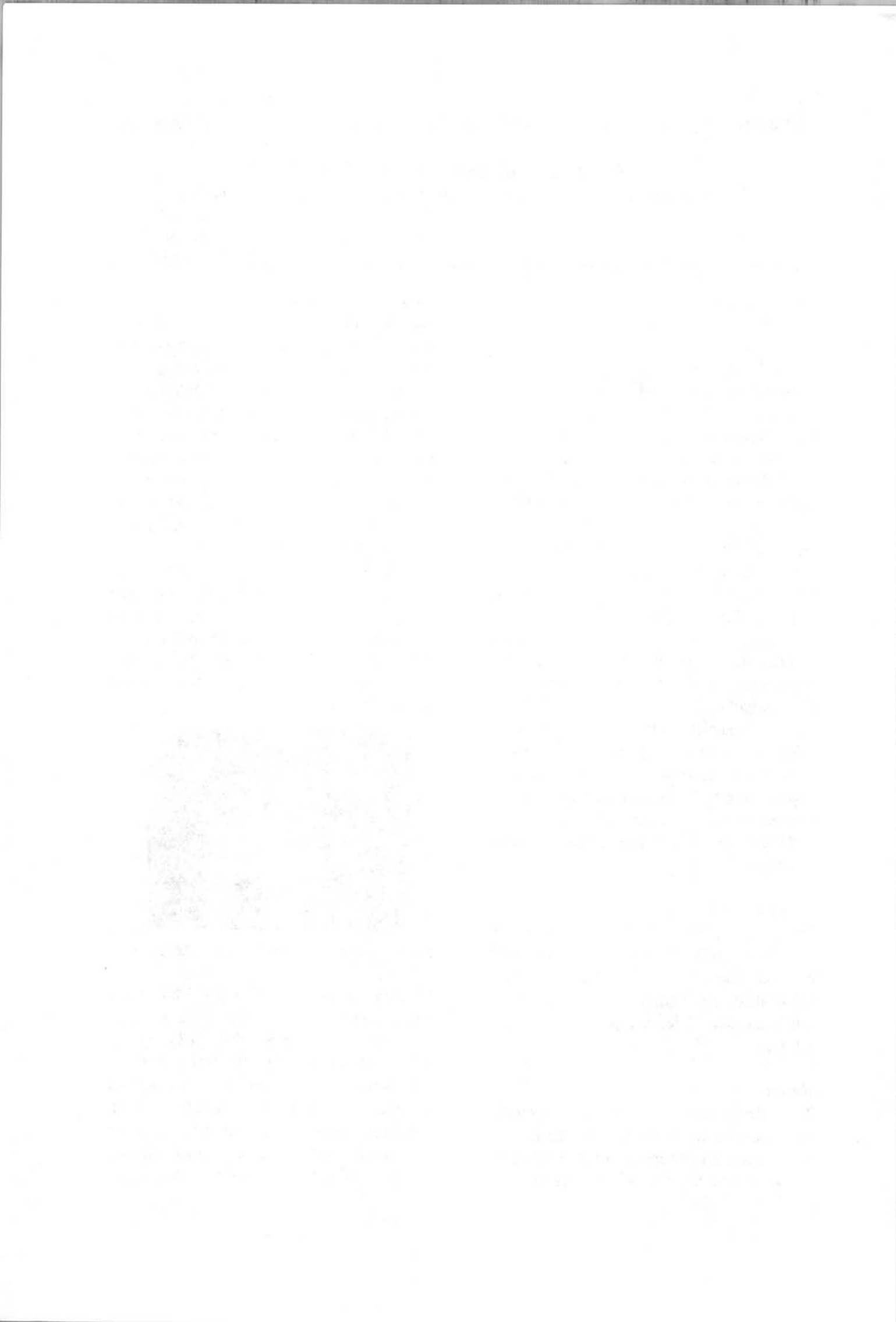


Fig. 1: Side view of corrosion under SiC layer.

In some areas Cr/Fe rich SiC-phases are formed where SiC deposition has a totally different morphology. The Cr/Fe island formation could, up to now, not be connected to the formation of cracks but there are strong indications. Future research will be focused on elucidating the effect of the substrate on the initial growth process and preventing the formation of cracks.





# In-situ Raman Spectroscopy During Laser-induced CVD of Silicon Thin Films

W.F.A. Besling, A. Goossens, and J. Schoonman

Laboratory for Applied Inorganic Chemistry, Delft University of Technology

E-mail: Besling@stm.tudelft.nl

tel: +31-15-2782637

## Introduction

In order to obtain a detailed understanding of gas phase reactions and, in particular, Chemical Vapor Deposition (CVD) processes, diagnostic techniques are required for *in situ* identification of the reacting gases and determination of their concentration and temperature. Raman scattering can meet these requirements and has been used to identify molecules and measure their concentration gradients and temperature with a high spatial resolution inside a Laser CVD reactor.

## Experimental setup

A pulsed, frequency doubled (0.45 W, 523 nm) Spectra Physics Nd-YLF laser has been used to generate the Raman effect.

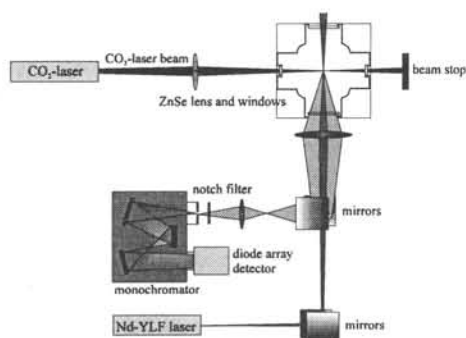


Fig. 1: Raman setup in backscatter configuration.

The laser beam is focused in the reaction zone by a  $f/2.0$ , 150 mm lens. The back scattered light is collected with the same lens and focused on the entrance slit of a monochromator (Spex 340A  $f/5.9$ ). In order to suppress background optical noise, a gated diode array detector is used (Fig 1). A 150 W tunable continuous wave  $\text{CO}_2$  laser (Edinburgh PL6) is used to heat the reactants (99% silane) and to initiate the reaction. The  $\text{CO}_2$  laser beam is directed

parallel to the substrate and intersects the reactant gas flow perpendicularly. Nitrogen and hydrogen are used as shield gases.

## Results and Discussion

Silicon thin films are obtained at reactor pressures of 20 torr and substrate temperatures of  $200^\circ\text{C}$  during  $\text{CO}_2$  laser excitation. The growth rate is about 10 nm/min. In Fig. 2 the Raman spectra are shown with and without  $\text{CO}_2$  laser excitation. Switching on the  $\text{CO}_2$  laser, the

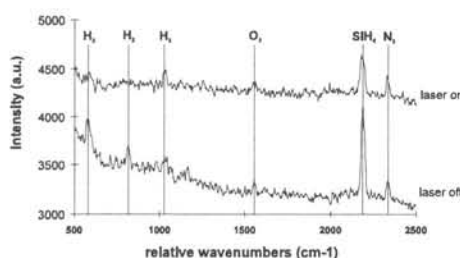


Fig. 2: Raman spectra of silane (20 sccm),  $\text{H}_2$  (20 sccm), and  $\text{N}_2$  (1.3 slm), at 20 torr.

silane peak height decreases due to a decrease in species number density. This can be explained by the increase in temperature or by decomposition of silane. However, no new Raman peaks are visible, so we must conclude that possible decomposition products ( $\text{SiH}_2$ ) have a concentration below the detection limit. The hydrogen peak at  $587\text{ cm}^{-1}$  has disappeared but the one at  $1046\text{ cm}^{-1}$  has the same intensity indicating the presence of higher excited rotational levels. The gas temperature in the reaction zone is estimated to be between  $6.10^2\text{ K}$  and  $1.10^3\text{ K}$ . Present research is directed towards improvement of the signal-to-noise ratio in order to elucidate the chemistry of laser CVD processes.



# Morphology Control of Thin $\text{LiCoO}_2$ Films Fabricated Using Electrostatic Spray Deposition (ESD) Technique

Chunhua Chen, Erik M. Kelder, Paul J.J.M. van der Put, and J. Schoonman

Laboratory for Applied Inorganic Chemistry, Delft University of Technology,  
Julianalaan 136, 2628 BL Delft, The Netherlands

## OBJECTIVE OF THIS STUDY

Establishment of the relationship between the morphologies of ESD-deposited  $\text{LiCoO}_2$  thin films and deposition conditions, including deposition duration, deposition temperature, precursor solution concentration, electric field strength, substrate, and solvent composition.

## EXPERIMENTAL

Table. ESD conditions of  $\text{LiCoO}_2$  thin films

Precursors	Solvent	Concentration	Voltage	Deposition temp.	substrate
$\text{Li(OAc)} \cdot 2\text{H}_2\text{O}$ , $\text{Co(NO}_3)_2 \cdot 6\text{H}_2\text{O}$ or $\text{Co(OAc)}_2 \cdot 4\text{H}_2\text{O}$	$\text{C}_2\text{H}_5\text{OH}$ or with butyl carbitol	0.003 M to 0.05 M	+8 kV to +15 kV	200°C to 500°C	S.S., Al, $\text{Al}_2\text{O}_3$ , YSZ

## RESULTS

### • Four types of $\text{LiCoO}_2$ layer morphology (Fig.1)



Fig. 1 Four types of layer morphology obtained by ESD. I, dense layer; II, dense layer with incorporated particles; III, porous top layer with dense bottom layer; IV, fractal-like porous layer.

### • Effect of deposition time (Fig.2)

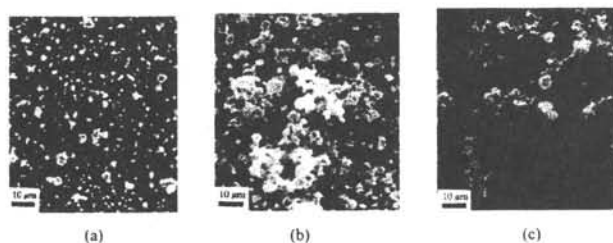


Fig. 2 Surface morphologies of layers deposited at 340°C for different deposition times: (a) 1; (b) 3; (c) 6 h. Precursor solution, 0.04 M  $\text{Li(OAc)} \cdot 2\text{H}_2\text{O}$  +  $\text{Co(NO}_3)_2 \cdot 6\text{H}_2\text{O}$  ethanol solution; substrate, stainless steel; applied voltage, 11 kV. With increasing the deposition time, the  $\text{LiCoO}_2$  layer becomes porous.

### • Effect of deposition temperature (Fig.3)

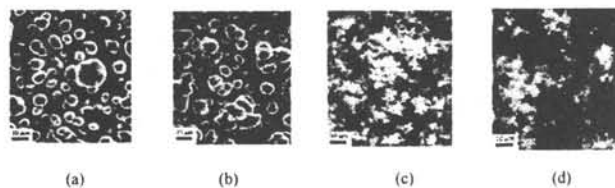


Fig.3 Surface morphologies of layers deposited at different temperatures for 6 h: (a) 230; (b) 280; (c) 400; (d) 500°C. Other conditions are the same as in Fig. 2 except that Pt was used as substrate for (d). With increasing deposition temperature, the  $\text{LiCoO}_2$  layer becomes porous.

### • Effect of precursor solution concentration (Fig.4)



Fig 4 Surface morphologies of layers deposited at 350°C for 2 h with solutions of different concentrations: (a) 0.0038; (b) 0.010 M. Other conditions are the same as in Fig.2. The layer morphology is slightly influenced by the precursor solution concentration.

### • Effect of electric field strength (Fig.5)

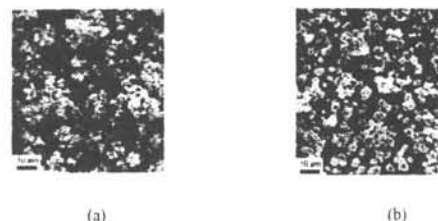


Fig.5 Surface morphologies of layers deposited at 350°C for 4 h with applied voltages: (a) 8; (b) 15 kV. A lower voltage resulted in a more porous morphology.

### • Effect of substrate (Fig.6)

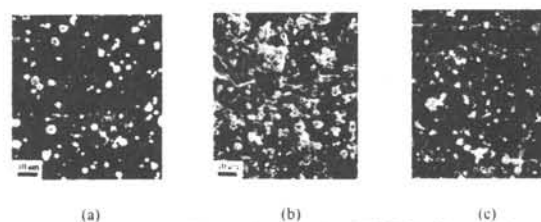


Fig.6 Surface morphologies of layers deposited at 350°C for 2 h on substrates: (a) Al (smooth); (b)  $\text{Al}_2\text{O}_3$  (rough); (c) YSZ (smooth). The original roughness of a substrate affects markedly the final layer morphology.

### • Effect of solvent (Fig.7)

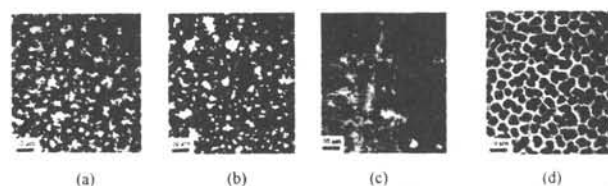


Fig.7 Surface morphologies of layers deposited using precursor solutions with solvent compositions: (a) 100 vol% ethanol, at 450°C for 2 h; (b) 67 vol% ethanol + 33 vol% butyl carbitol, at 450°C for 2 h; (c) 50 vol% ethanol + 50 vol% butyl carbitol at 250°C for 4 h; (d) 15 vol% ethanol + 85 vol% butyl carbitol (0.005 M  $\text{Li(OAc)} \cdot 2\text{H}_2\text{O}$  +  $\text{Co(OAc)}_2 \cdot 4\text{H}_2\text{O}$ ), at 230°C for 2 h.

## SUMMARY

The electrostatic spray deposition (ESD) technique opens the opportunity to control the morphology of a layer. Many factors may influence the morphology. The substrate temperature and the solvent composition play the most important role.

This study is financed by SON/NWO.

20

21

22

23

24

25

26

27

28

29

30

31

32

33

34

35

36

37

# Effects of Additives in Electrospraying for Materials Preparation

C.H. Chen, E.M. Kelder, and J. Schoonman

Laboratory for Applied Inorganic Chemistry, Delft University of Technology,  
Julianalaan 136, 2628 BL Delft, The Netherlands

Sponsor: NWO-SON

Tel: +31-15-2782637

E-mail: chunhua.chen@stm.tudelft.nl

## OBJECTIVE OF THE STUDY

Investigation of the effects of additives in precursor solutions on the morphologies of ceramic thin films and powders synthesized by electrospaying technique.

## EXPERIMENTAL

### • Materials:

#### TiO<sub>2</sub> thin films:

via 0.005M Ti(OPr)<sub>3</sub> in ethanol (ET) + butyl carbitol (BC); deposited at 240°C on Al substrate.

#### ZrO<sub>2</sub> powders:

via 0.05M Zr(AcAc)<sub>4</sub> in ET; collected on a heated Al plate (340°C).

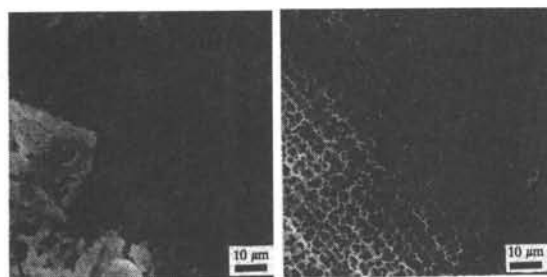
### • Additives:

Solution chemistry modifier: HAc.

Conductivity enhancement additive: NH<sub>4</sub>NO<sub>3</sub>

## RESULTS

### • TiO<sub>2</sub> thin-film deposition and solution chemistry modifier (Fig.1)

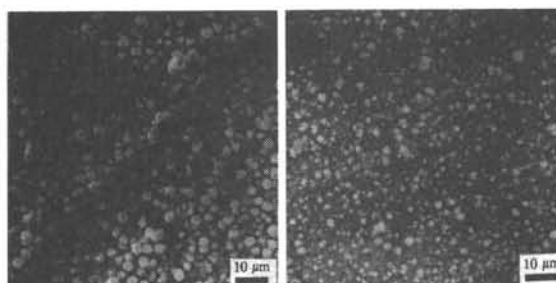


(a)

(b)

Fig.1 TiO<sub>2</sub> thin films from precursor solutions containing different amounts of HAc: (a) 0 vol%; and (b) 30 vol%.

### • ZrO<sub>2</sub> powder production and conductivity enhancement additive (Fig.2)

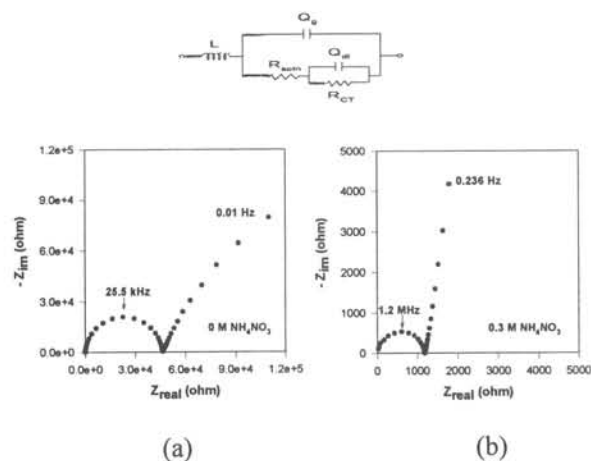


(a)

(b)

Fig.2 ZrO<sub>2</sub> powders from precursor solutions containing different amounts of NH<sub>4</sub>NO<sub>3</sub>: (a) 0 M; and (b) 0.03M.

### • Impedance spectra of Zr-precursor solutions (Fig.3)



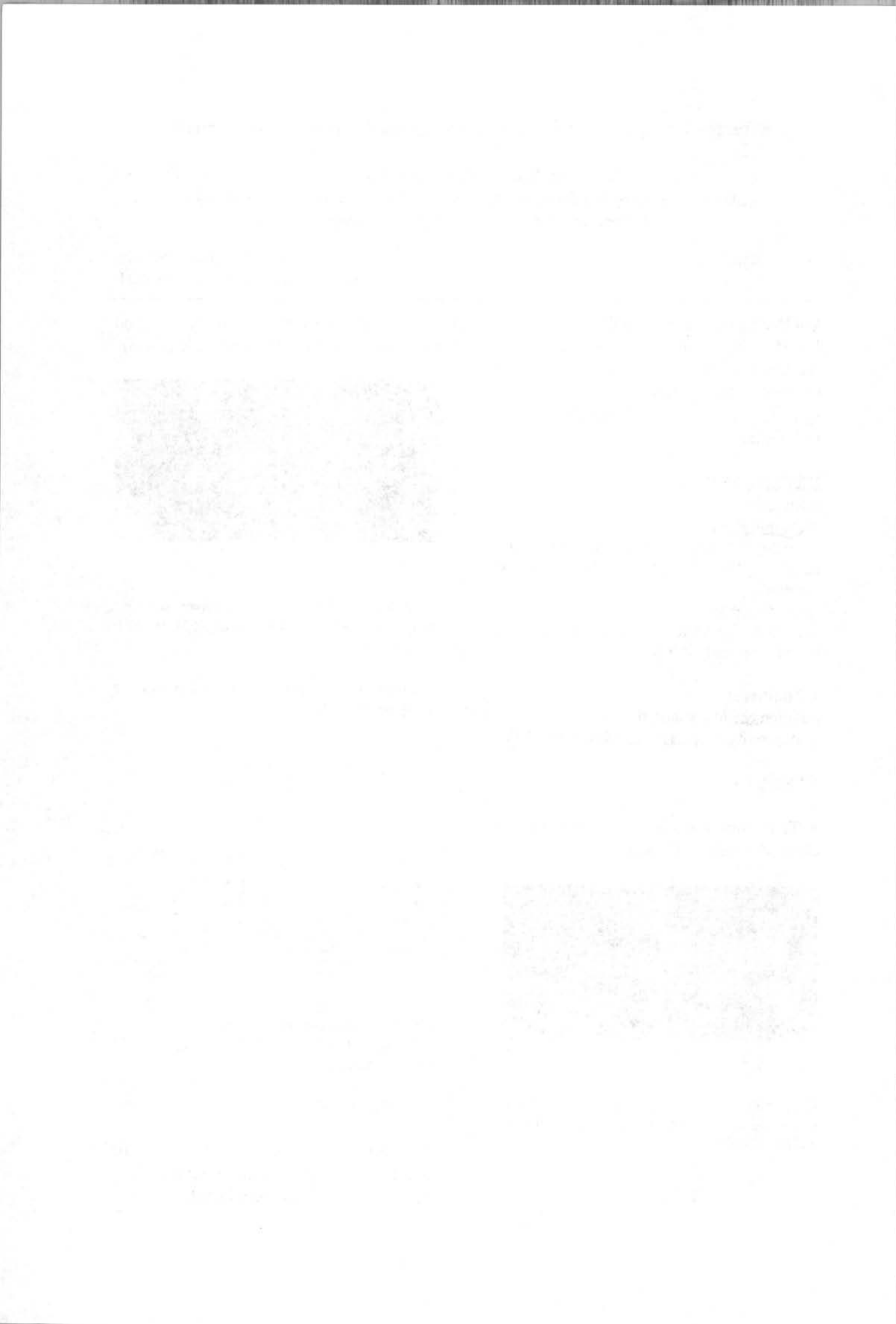
(a)

(b)

Fig.3 Impedance spectra of Zr-precursor solutions containing 0 M (a) and 0.3 M (b) NH<sub>4</sub>NO<sub>3</sub>, and their equivalent circuit.

## CONCLUSION

By using different additives, the morphologies of electrospaying-derived ceramic materials can be tailored.



# Chemical gas sensor array for the detection of NO<sub>x</sub> and CO.

M.H.J. Emond, R.C. van Landschoot and J. Schoonman

Laboratory for Applied Inorganic Chemistry

Faculty of Chemical Technology and Materials Science

Tel: +31-15-2782670

e-mail: M.H.J.Emond@STM.TUdelft.nl

## Introduction

Taguchi-type gas sensors are based on semiconducting oxide films. Gas adsorption affects the electronic charge density and thereby changes the electrical properties of the oxide film.

In our Laboratory we have successfully improved the selectivity by using two-phase mixtures of n-type and p-type semiconducting oxides and inert nonconducting metal oxides.

This concept is used to design an array of Taguchi-type gas sensors, based on different electrical composites, in order to analyse complex gas mixtures in a single measurement.

## Material selection

In horticulture the CO<sub>2</sub> from exhaust gases is introduced into greenhouses as a fertiliser. This requires the exhaust gases to be cleaned from NO<sub>x</sub>, CO, and C<sub>2</sub>H<sub>4</sub>. Therefore, reliable gas sensors are required for the detection of these gases. In the present design study emphasis is put on the quantitative detection of NO<sub>x</sub> and CO.

The sensitivities of SnO<sub>2</sub> and several electrical composites are presented in Table 1.

	NO	NO <sub>2</sub>	CO
SnO <sub>2</sub>	1.43	0.49	1.86
Al <sub>2</sub> O <sub>3</sub> -V <sub>2</sub> O <sub>5</sub>	1.54	1.71	0.09
Al <sub>2</sub> O <sub>3</sub> -ZnO	4.37	5.39	6.08
SnO <sub>2</sub> -ZnO	0.53	0.54	5.04
V <sub>2</sub> O <sub>5</sub> -ZnO	1.41	1.61	1.00

**Table 1:** The sensitivity of composites to NO<sub>x</sub> and CO.

The sensitivity is defined as the relative conductivity change with respect to the conductivity in air.

The following electrical composites have been selected:

For NO<sub>x</sub>: ZnO-V<sub>2</sub>O<sub>5</sub>, a p-n composite.

For CO: ZnO-SnO<sub>2</sub>, a n-n composite.

## Experimental

Thin films of the active sensor components are deposited on non-conducting ceramic substrates using Electrostatic Spray Deposition (ESD), a recently in our laboratory developed cheap and efficient deposition technique for electroceramics. With this technique it is very easy to control the microstructure and morphology of thin layers of electroceramics.

## Results and future research

Zn(OOCCH<sub>3</sub>)<sub>2</sub>·2H<sub>2</sub>O was used as a precursor, and dissolved in ethanol (0.1 M). Figure 1 shows the surface morphology of ZnO layer on Al<sub>2</sub>O<sub>3</sub> deposited at 400°C. The films are porous with a grain size of about 5 μm.



**Figure 1:** SEM-micrograph

Current research is focused on ESD of SnO<sub>2</sub>, V<sub>2</sub>O<sub>5</sub>, and the composites, as well as on array structures.

THE UNIVERSITY OF CHICAGO  
DEPARTMENT OF THE HISTORY OF ARTS  
AND ARCHITECTURE

1950-1951  
1952-1953

1954-1955  
1956-1957

1958-1959  
1960-1961

1962-1963  
1964-1965

1966-1967  
1968-1969

1970-1971  
1972-1973

1974-1975  
1976-1977

1978-1979  
1980-1981

1982-1983  
1984-1985

1986-1987  
1988-1989

1990-1991  
1992-1993

1994-1995  
1996-1997

1998-1999  
2000-2001

2002-2003  
2004-2005

2006-2007  
2008-2009

2010-2011  
2012-2013

2014-2015  
2016-2017

2018-2019  
2020-2021

2022-2023  
2024-2025

2026-2027  
2028-2029

2030-2031  
2032-2033



## RUPTURE OF THIN LIQUID FILMS

AIO : L.J. Evers

Sponsor : TUD

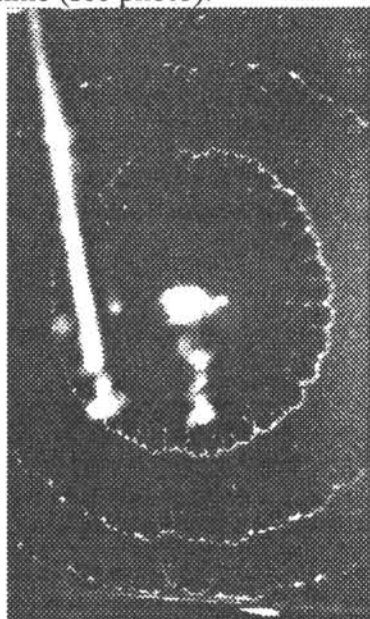
☎ 015-2782658

✉ l.evers@stm.tudelft.nl



Investigations on the bursting of vertical thin liquid films stabilized by surfactants have been made. The use of high speed flash photography enables us to determine the bursting velocity.

Because rapid flashes at constant intervals were used the evolution of the burst could be followed. This leads to the observation that Newton-black films of sodium dodecyl sulphate solutions (SDS) and some other liquids show retardation of the expansion rate in time (see photo).



This is in contradiction with the generally accepted idea (expressed in Culick's formula  $v = [(2\gamma)/(\rho\delta)]^{1/2}$ , where  $v$  is the rate of expansion,  $\delta$  is the thickness of the film,  $\rho$  its density and  $\gamma$  its surface tension) that the rate of expansion of a hole in a thin liquid film must be constant due to conservation of momentum.

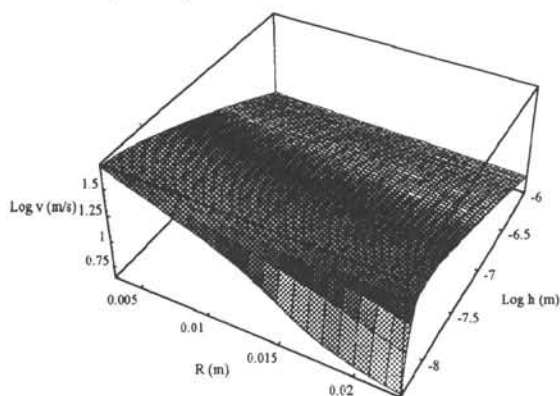
Indeed thick SDS films, including the common-black film show a constant bursting rate. The Newton-black film bursts in an anomalous, retarded fashion. The rim of the hole is not toroidal in these films. It has a scalloped appearance, small droplets issuing from the loci where the

motion of the rim is the slowest. Liquid films drawn from a visco-elastic liquid also show a retardation. Experiments show a smooth transition of bursting behaviour going from thicker visco-elastic films to the thinnest, Newton-black film, whereas for a SDS solution the transition in mechanical behaviour is abrupt.

This demonstrates that the thinnest SDS film, though formed from a Newtonian liquid, has a complex storage modulus which can be compared with that of visco-elastic films. The bursting behaviour, which is observed in the Newton-black film, reflects non-Newtonian (visco-elastic) properties. It appears that very thin free liquid films of this kind are lyotropic liquid crystalline bilayers rather than a very thin film of liquid.

We extended the existing Culick theory (describing 'Newtonian bursting behaviour') on the rather general case of visco-elastic liquid films. In the figure the result of this extended theory is showed for an SDS solution which shows Newtonian behaviour for films thicker than 10 nm. For thinner films (Newton-black films, see also photo) visco-elastic behaviour becomes clear; a decrease in rupture velocity for increasing hole size.

The Rupture Velocity as a Function of Hole Radius and Film Thickness (SDS solution)





# Cuprisation of polyetherimide by Chemical Vapour Deposition

*M.L.H. ter Heerdt, P.J.J.M. van der Put, and J. Schoonman*

*Laboratory for Applied Inorganic Chemistry  
Faculty of Chemical Technology and Materials Science*

Sponsor: IOP Surface Technology

Tel: + 31-15-2782637

e-mail: M.L.H.terHeerdt@STM.TUdelft.NL

## Introduction

This study is performed in the framework of an IOP Surface Technology project, titled "Functional metallic layers on plastics".

Metallisation of plastics nowadays is used in several applications like decoration and industrial products. One of the ways to metallise materials is Chemical Vapour Deposition (CVD), normally a too high temperature process for plastics.

Using the copper precursor copper(I)hexafluoroacetylacetonate vinyltrimethylsilane (Cu(hfac)VTMS) plastics like polyetherimide (PEI) can be metallised at 130 °C already.

## Experimental

CVD experiments were carried out using ULTEM 1000 and ULTEM 2400, provided by GE Plastics, as substrates in a home-made cold-wall reactor.

Experimental conditions are shown in table 1. Hydrogen is used as a coreactant, to enhance layer quality.

**Tab. 1** *Process conditions*

$T_{\text{precursor}}$	45 °C
$T_{\text{substrate}}$	125-175 °C
$P_{\text{reactor}}$	5 Torr
$\Phi_{\text{nitrogen, precursor}}$	70 sccm
$\Phi_{\text{hydrogen}}$	90 sccm

Resistance measurements were performed according to the Van der Pauw method. From this sheet resistance, the bulk resistance could be calculated using the layer thickness measured with a Tencor P-10 Surface Profiler.

## Results

The growth rates on ULTEM 1000 show an Arrhenius like behaviour. Growth rates of up to 100 nm/min were measured.

According to the resistances calculated ( $\rho \sim 5\rho_{\text{bulk}}$ ) the copper layers were of good quality.

In figure 1 a SEM picture of a typical copper layer is shown. The different stadia of layer growth can be seen.

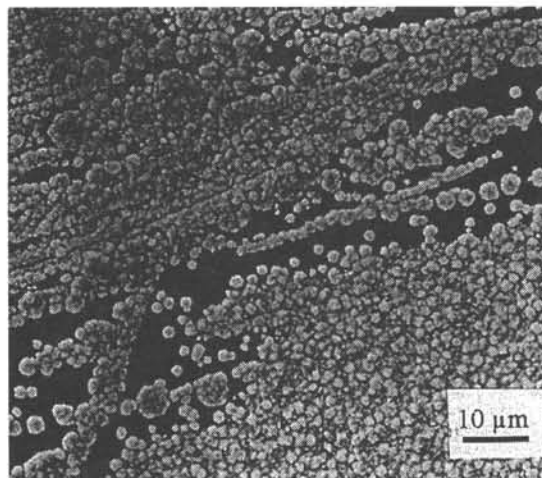
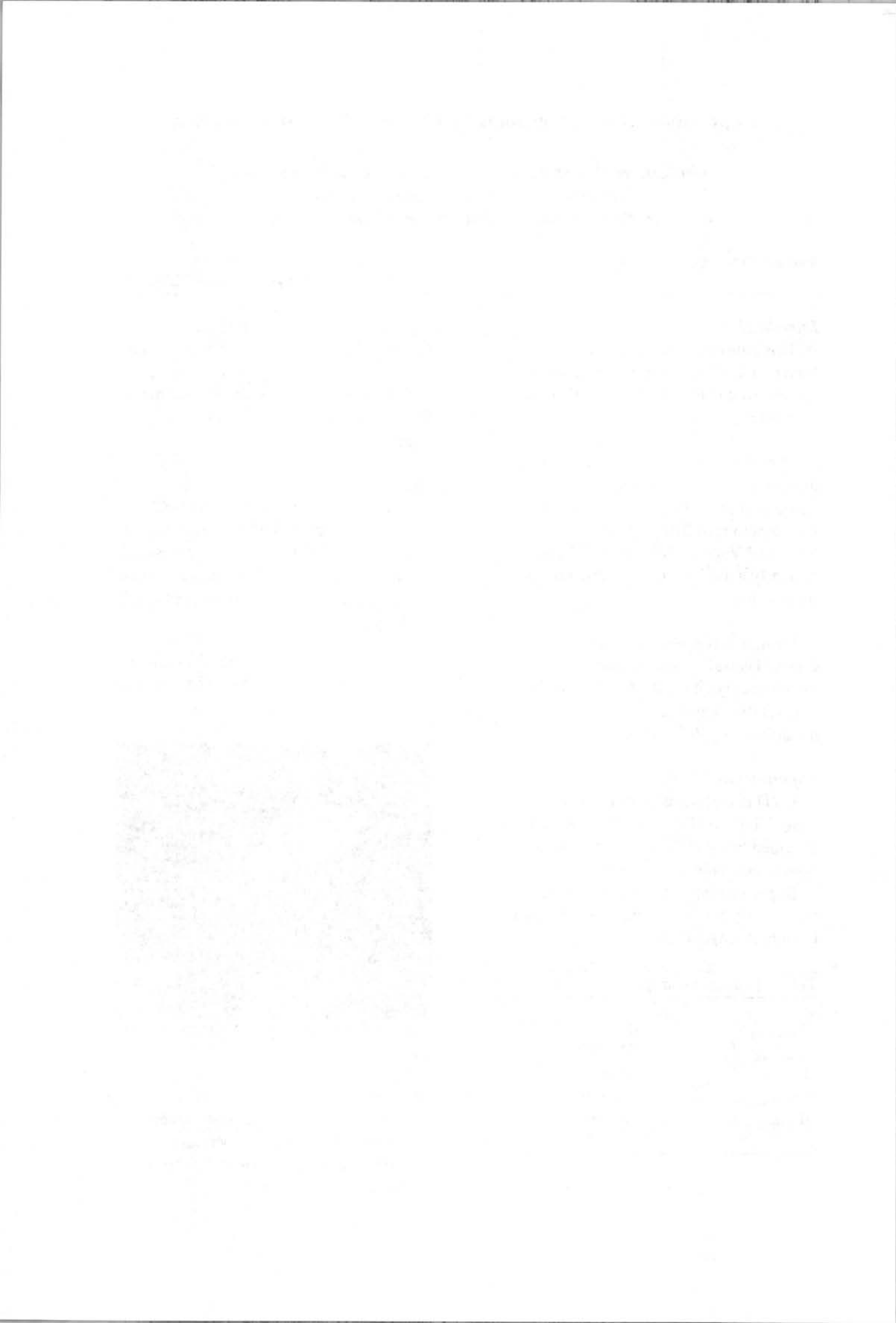


**Fig. 1** *SEM photograph of a copper layer on ULTEM 1000*

## Conclusions

Deposition of good quality copper layers onto PEI at low temperatures appears to be possible. Growth rates are acceptable.



# The Catalytic Sensor for Detection of Natural Gas

L.N. van Rij, R.C. van Landschoot, and J. Schoonman

Laboratory for Applied Inorganic Chemistry, Delft University of Technology

Julianalaan 136, 2628 BL, Delft, The Netherlands

Tel: +31 (0) 15 2782676

e-mail: L.N.vanRij@stm.tudelft.nl

## Introduction

The sensor consists of the solid proton conducting electrolyte  $\text{SrCe}_{0.95}\text{Yb}_{0.05}\text{O}_{3-\alpha}$ , a catalytic electrode (Ni, Ru, or Rh), and a counter electrode (Au or Pt), which has a lower catalytic activity than the catalytic electrode (Figure 1)

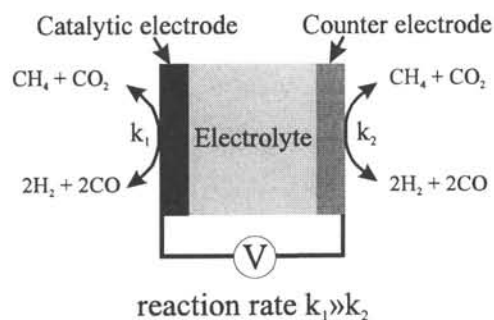


**Figure 1:** Schematic representation of the Catalytic Asymmetrical Nernst-type Methane sensor

The difference in catalytic activity creates a chemical potential gradient in hydrogen across the solid electrolyte. This causes a potential difference across the cell, which is a measure for the amount of methane present.

This method of detection can also be used for ethane and probably also for other hydrocarbons, like propane.

## Results

A  $\text{Ru}/\text{SrCe}_{0.95}\text{Yb}_{0.05}\text{O}_{3-\alpha}/\text{Pt}$  cell is tested in a  $\text{CH}_4/\text{CO}_2$  mixture, with a constant  $\text{CO}_2$  concentration of 5 vol.%, while the hydrocarbon concentration is varied. A current of  $50\text{ }\mu\text{A}$  is placed across the cell, flowing from the catalytic electrode to the counter electrode, to create an extra driving force for proton conductance through the cell. The operating temperature of the sensor is  $500\text{ }^\circ\text{C}$ .

The results are given in Figure 2.

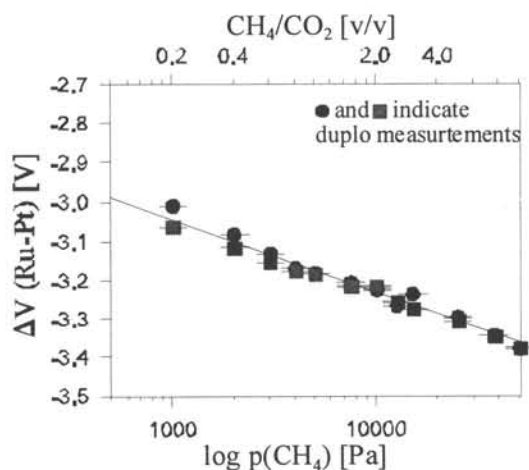


**Figure 2:** The influence of the methane partial pressure on the potential of a  $\text{Ru}/\text{SrCe}_{0.95}\text{Yb}_{0.05}\text{O}_{3-\alpha}/\text{Pt}$  cell at  $500\text{ }^\circ\text{C}$



# Preparation of Zirconium Dioxide Powder by Flame-Assisted Ultrasonic Spray Pyrolysis (FAUSP)

*F.L. Yuan, C.H. Chen, E.M. Kelder, and J. Schoonman*  
*Laboratory for Applied Inorganic Chemistry, Delft University of Technology,*  
*Julianalaan 136, 2628 BL Delft, The Netherlands*

Sponsor: NUFFIC

Tel: +31-15-2788452  
E-mail: F.Yuan@stm.tudelft.nl

## Introduction

A new technique, i.e. Flame-Assisted Ultrasonic Spray Pyrolysis (FAUSP), has been developed recently in our laboratory to prepare ceramic powders. Zirconia was selected as a model material in this study.

The FAUSP has following advantages:

- Simple, inexpensive equipment
- Easy to operation
- Ambient atmosphere
- Fine and narrow-distributed particle sizes.

## Experiment

Schematic diagram of the experimental set-up is shown in Fig.1. Powders are produced by self-sustained burning of the aerosol at the outlet of the nozzle and collected on a stainless steel plate. Other details are:

- Nebulizer: Ultra-bel 2000 (1.63MHz)
- Precursor:  $\text{Zr}(\text{i-C}_3\text{H}_7\text{O})_4$
- Solvent: ethanol (96%) +  $\text{H}_2\text{O}$  (4%)
- Carrier gas : air

## Results and conclusion

SEM analysis of  $\text{ZrO}_2$  powder shows that the particles were spherical. It has a narrow particle-size distribution in micron- or submicron- meter range, depending on the concentration of the precursor solutions. A smaller concentration leads to a smaller particle size. A SEM micrograph is shown in Fig.2.

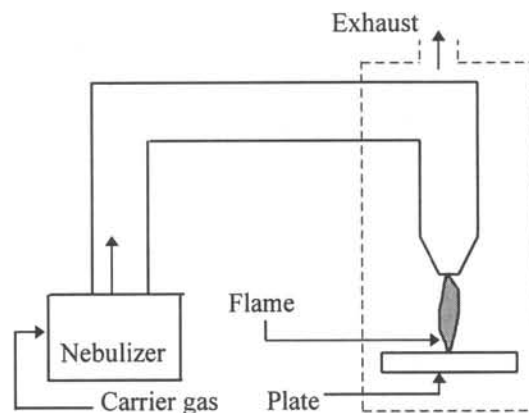


Fig. 1. Schematic diagram of the FAUSP set-up

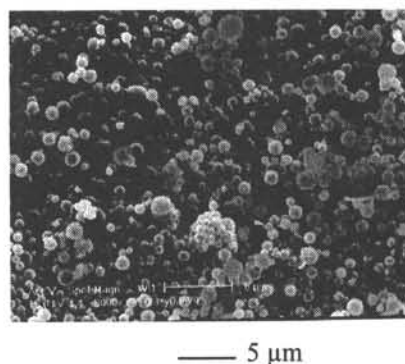
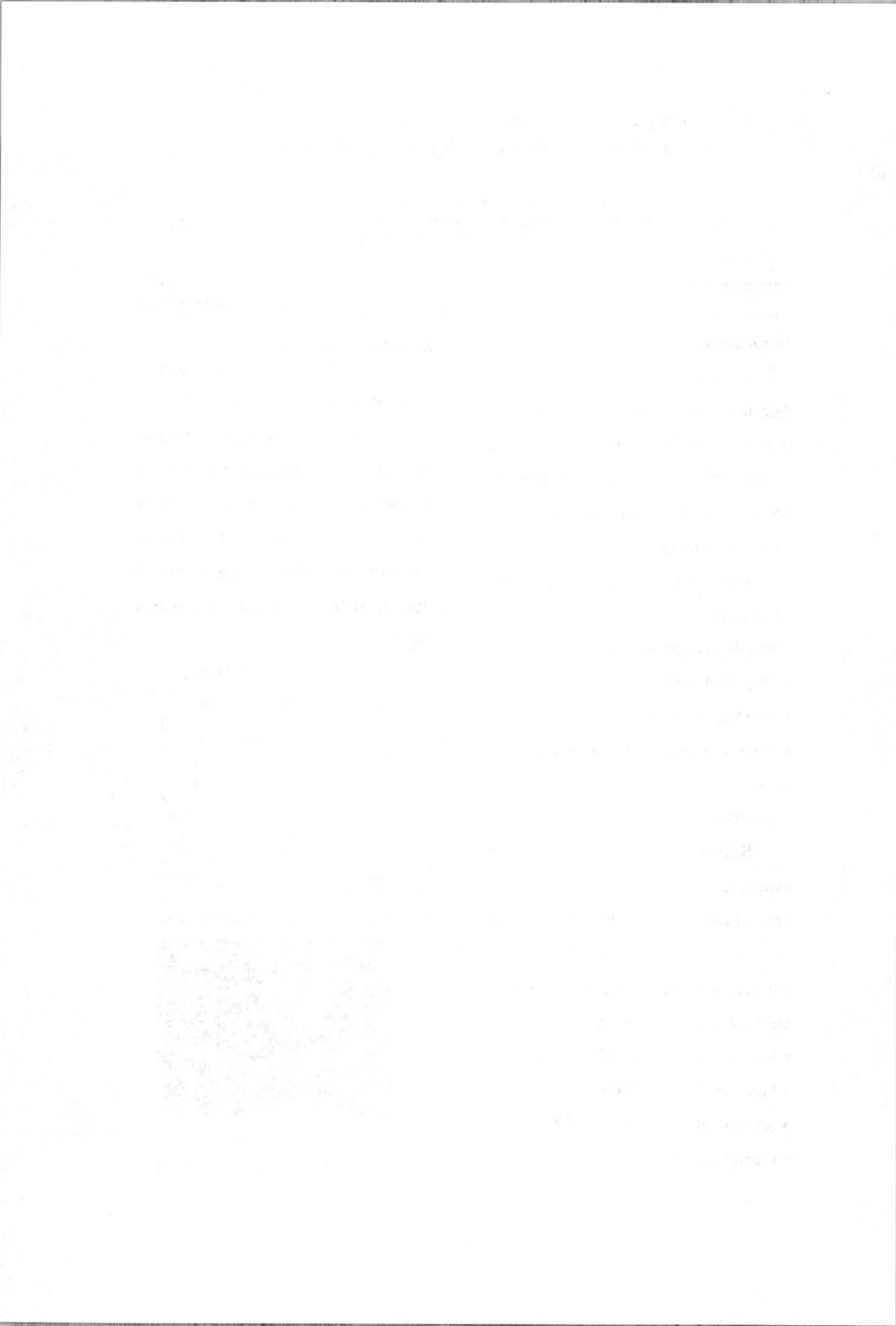


Fig. 2. SEM of  $\text{ZrO}_2$  powder (via 0.2 M sol)





# Industrial Catalysis

Group leader: Prof.dr. J.A. Moulijn  
Address: Delft University of Technology  
Faculty of Chemical Technology and Materials  
Science  
Julianalaan 136  
NL 2628 BL Delft  
+31-15-278 6725  
J.A.Moulijn@STM.TUdelft.NL  
+31-15-278 4452



fax:



# Quasi In-Situ XPS Characterisation of Different Nickel Species in NiW/ $\gamma$ -Al<sub>2</sub>O<sub>3</sub> Hydrotreating Catalysts Upon Sulfiding.

Hank Reinhoudt, Rafaël Mariscal, Dick van Langeveld and Jacob Moulijn

Section of Industrial Catalysis, Faculty of Chemical Technology and Material Science

Sponsor: NWO/SON

Tel: 31-15-2784395

E-mail: H.Reinhoudt@stm.tudelft.nl

## Introduction

This XPS study is part of a research program with aims to define design rules for hydrotreating catalysts. These catalysts are used in oil refineries to upgrade oil fractions, for example by reducing the sulfur content of it. From earlier work it was found that NiW/ $\gamma$ -Al<sub>2</sub>O<sub>3</sub> catalysts are promising catalysts, especially in the deep HDS of gasoil. Moreover, it appeared that for NiW/ $\gamma$ -Al<sub>2</sub>O<sub>3</sub> the activation, i.e. the temperature of sulfiding, plays a crucial role in the final activity and selectivity.

An extensive characterisation by TPS, FTIR (NO), and Raman was done to study the genesis of various W and Ni species upon sulfiding. To acquire quantitative information on the behaviour of Ni, this quasi in-situ XPS study was done.

## Experimental

A Ni(1.2 wt%)W(15.2 wt%)/ $\gamma$ -Al<sub>2</sub>O<sub>3</sub> catalyst was prepared by pore-volume impregnation. Two batches were calcined at 673 and 823 K in air. The catalysts were sulfided in 10% H<sub>2</sub>S/H<sub>2</sub> at various temperatures for 1 h and transferred into

the XPS machine without exposure to (wet) air.

## Results and discussion

The peak position of the Ni 2p<sub>3/2</sub> emission line was corrected by referencing to the Al 2p line at 74.7 eV. From a systematic deconvolution of the Ni 2p<sub>3/2</sub> line in a series of sulfided NiW/ $\gamma$ -Al<sub>2</sub>O<sub>3</sub> catalysts, combined with results from other techniques, it was found that six distinct Ni-species are present in different stages of sulfiding. The final results are collected in figure 1. for the 673 K calcined catalyst.

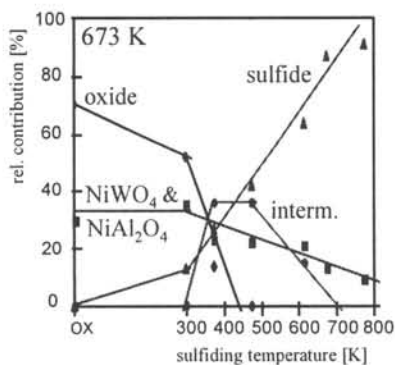


**Fig 1.** The relative amounts of the various Ni species in NiW/ $\gamma$ -Al<sub>2</sub>O<sub>3</sub> calcined at 673 K as a function of the sulfiding temperatures.

It appears that three species are present in the oxidic catalyst precursor which can be identified as NiO, NiAl<sub>2</sub>O<sub>4</sub> and NiWO<sub>4</sub>. After sulfiding at room temperature a NiS species is present. After sulfiding at about 500 K, an intermediate type of Ni appears which disappears again at higher sulfiding temperatures. The detailed nature of it is not yet clear.

The binding energies of the Ni species in the catalyst calcined at 823 K upon different sulfiding temperatures are shown in figure 2.

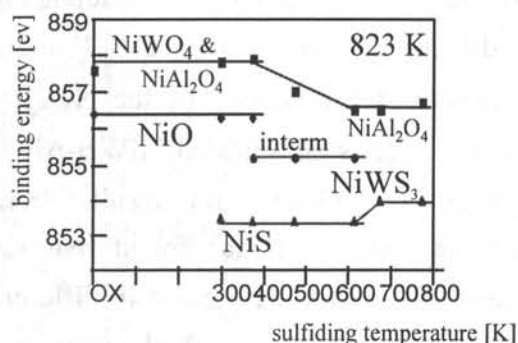


**Fig. 2.** The binding energy of the Ni-species in NiW/ $\gamma$ -Al<sub>2</sub>O<sub>3</sub> calcined at 823 as a function of the sulfiding temperature.

Most important observation from figure 2 is the distinct shift of the binding energy of the Ni-sulfide species upon sulfiding at temperatures above 673 K. This shift is interpreted as a redistribution of Ni along WS<sub>2</sub> slabs which are formed during sulfiding at 673 K and higher temperatures.

### Conclusions

The sulfiding behaviour of Ni in a NiW/ $\gamma$ -Al<sub>2</sub>O<sub>3</sub> catalyst has been studied by quasi in-situ XPS analysis. By a systematic deconvolution of the Ni 2p<sub>3/2</sub> emission line of a series of sulfided NiW/ $\gamma$ -Al<sub>2</sub>O<sub>3</sub> catalysts, it appeared that six different Ni species are present in the various stages of sulfiding.

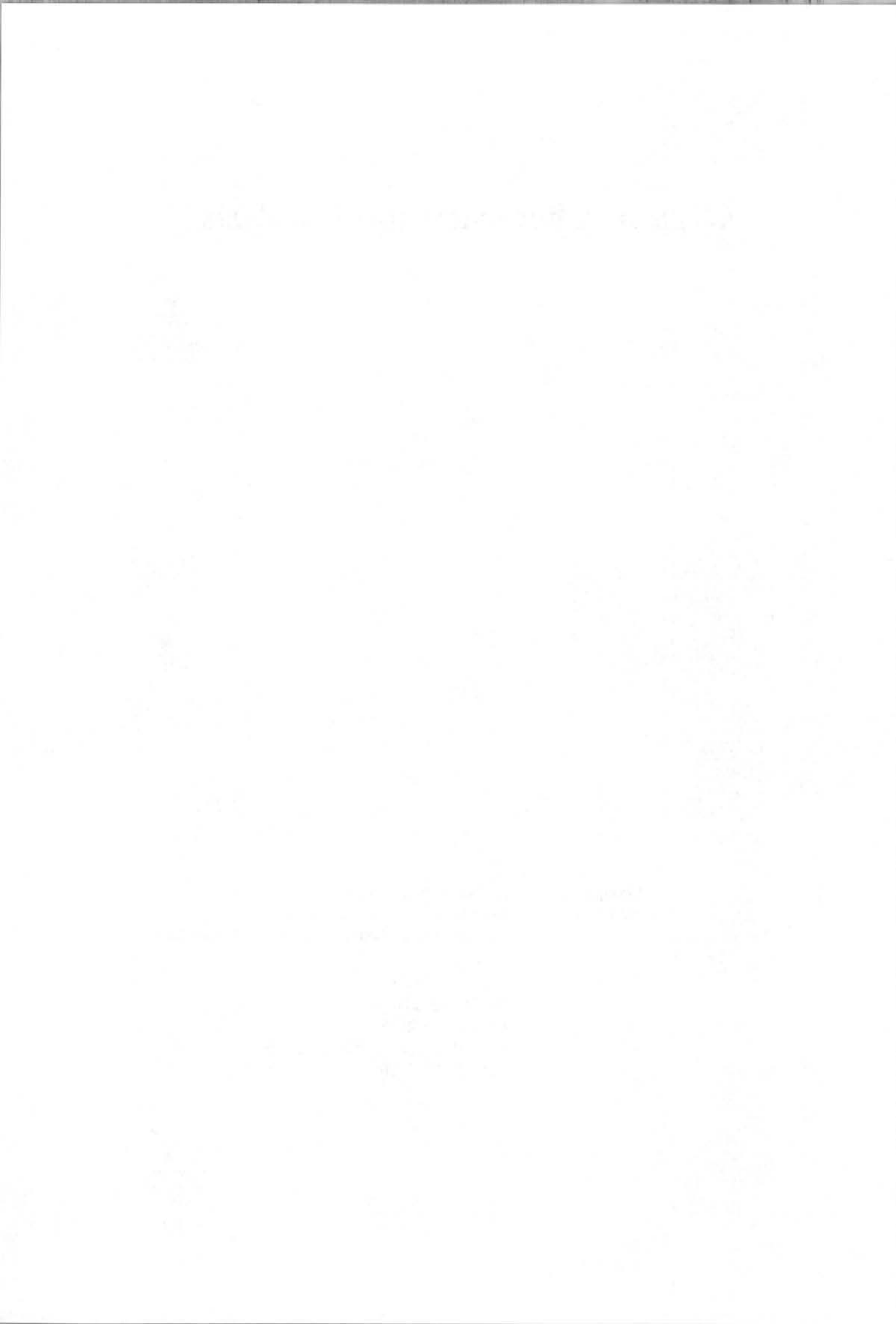
Quasi in-situ XPS can be used to obtain quantitative information about the presence and the state of metal oxides and sulfides in heterogeneous catalysts which can contribute to a better understanding of their sulfiding behaviour.

# Organic Chemistry and Catalysis

Group leader: Prof.dr. H. van Bakkum  
Address: Delft University of Technology  
Faculty of Chemical Technology and Materials  
Science  
Julianalaan 136  
NL 2628 BL Delft  
+31-15-278 2603  
H.vanBakkum@STM.TU Delft.NL  
+31-15-278 4700



fax:



# Design of a Zeolite-based Pyroelectric Thin Film Calorimeter

G.J. Klap<sup>a,b</sup>, J.C. Jansen<sup>b</sup>, H. van Bekkum<sup>b</sup>, M. Wübbenhorst<sup>a</sup>, and J. van Turnhout<sup>a</sup>  
Laboratories of Polymer Technology<sup>a</sup> and of Organic Chemistry & Catalysis<sup>b</sup>

Sponsor: FOM

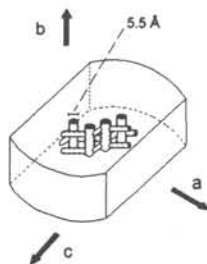
Tel: +31-15-278-2691  
E-mail: G.J.Klap@stm.tudelft.nl

## Introduction

Thin (oriented) zeolite layers have been grown on a metallized pyroelectric support. Using the photopyroelectric technique<sup>1</sup> this system acts as a micro calorimeter. In this configuration both the intrinsic thermal properties of the zeolite layer and thermal effects of an adsorbed phase can be determined.

## Zeolites

Zeolites have well-defined pores with molecular dimensions which form an excellent host for catalytic reactions and specific adsorption of several molecules. E.g. aligned p-nitroaniline molecules in  $\text{AlPO}_4\text{-5}$  show pyroelectric effects<sup>2</sup>.



Pore structure in a silicalite-1 crystal.

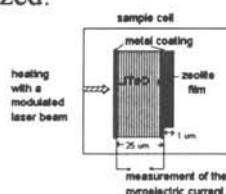
## Preparation of the zeolite film

A thin (1  $\mu\text{m}$ ) silicalite-1 film has been synthesized on one side of a Ni/Cr coated  $\text{LiTaO}_3$  wafer (25  $\mu\text{m}$ ). As a result of the synthesis conditions the crystals are oriented with the straight channels perpendicular to the support<sup>3</sup>.

The layers were analyzed with AFM, SEM (morphology) and XRD, FTIR (type, orientation).

## Photopyroelectric experiments

Photopyroelectric measurements have been performed on the described two-layer system by heating from the detector side with modulated laser light<sup>4</sup>. The frequency dependent pyroelectric current was measured and analyzed.



Set-up for photopyroelectric measurements.

For an as-synthesized silicalite-1 layer this results in a specific heat of 0.5 kJ/kgK (comparable with DSC results). The thermal conductivity is about 2 W/Km. As expected, this is significantly higher than values derived from powder measurements.

## Conclusions

Photopyroelectric analysis is a feasible method to determine the specific heat and thermal conductivity of thin zeolite films on a pyroelectric support. Measurements with adsorbed molecules are in progress. The described system may also be used as a calorimeter to study heats of reaction and adsorption in zeolite films.

## References

1. H. Coufal, in *New Characterization Techniques for thin Polymer Films* eds. H.M. Tong and L.T. Nguyen, New York, 1990 p. 231-264
2. F. Marlow et al. *J. Phys. Chem.* **98** (1994) 12315-12319.
3. J.C. Jansen et al., *Stud. Surf. Sci. Cat.* **85** (1994) 215-250.
4. G.J. Klap et al. *Stud. Surf. Sci. Cat.* **105c** (1997) 2093-2100.

1. The first part of the report deals with the general situation of the country and the progress of the work during the year. It is divided into two main sections: the first section deals with the general situation of the country and the progress of the work during the year, and the second section deals with the specific results of the work.

2. The second part of the report deals with the specific results of the work. It is divided into three main sections: the first section deals with the results of the work in the field of agriculture, the second section deals with the results of the work in the field of industry, and the third section deals with the results of the work in the field of commerce.

3. The third part of the report deals with the financial results of the work. It is divided into two main sections: the first section deals with the income of the work, and the second section deals with the expenditure of the work.

4. The fourth part of the report deals with the general conclusions of the work. It is divided into two main sections: the first section deals with the general conclusions of the work, and the second section deals with the specific conclusions of the work.

5. The fifth part of the report deals with the general recommendations of the work. It is divided into two main sections: the first section deals with the general recommendations of the work, and the second section deals with the specific recommendations of the work.



# Analyzing crystal surface roughness by Atomic Force Microscopy

J.H. Koegler, E.N. Coker, J.C. Jansen

Laboratory of Organic Chemistry and Catalysis

Delft University of Technology, Julianalaan 136, 2628 BL Delft, The Netherlands

Atomic Force Microscopy (AFM) is a powerful non-destructive technique to probe the physical external surface of catalysts. Images ranging in size from a few nanometer to several micrometers can be obtained. AFM measurements can be carried out under ambient conditions or submerged in a liquid.

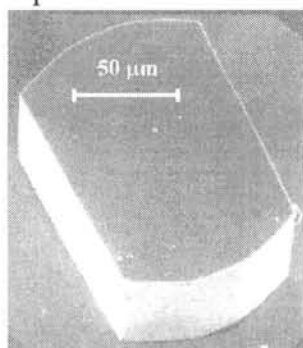


Figure 1:  
SEM of a zeolite MFI  
crystal

The effect of microgravity on zeolite crystallization was tested by preparing zeolite MFI on earth and in microgravity during Space Shuttle Flight STS-73 under otherwise iden-

tical conditions. Figure 1 shows a typical zeolite MFI crystal. The external surface of zeolite crystals grown on earth and in space are shown in Figure 2. The ground-based experiment shows a highly corrugated surface. The crystal grown under microgravity conditions, on the other hand, is much smoother. The roughness of both samples has been analysed:

	terrestrial	μ-gravity
area $R_a$	36.67	8.92
area RMS	49.59	11.17
avg. height (nm)	98.04	45.63

It may be speculated that the suppression of convection currents under microgravity conditions induces a smoother growth.

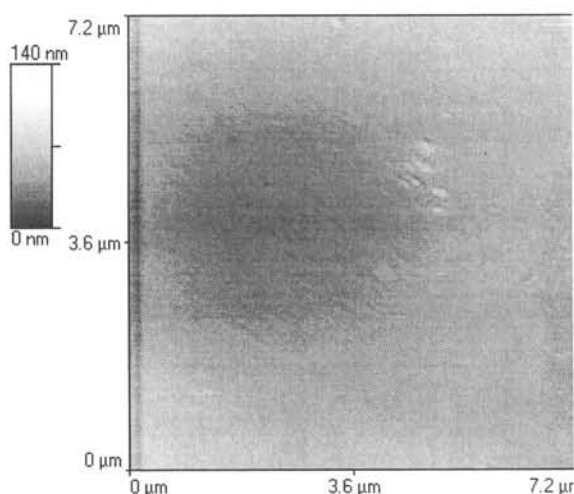
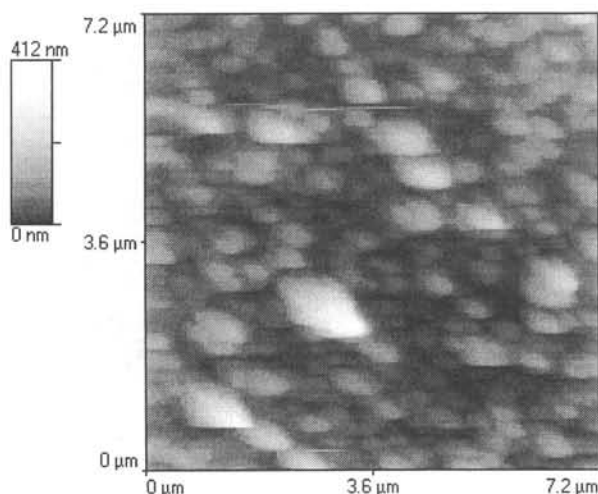


Figure 2: AFM image showing the surface roughness of MFI crystals grown on earth (left) and under microgravity conditions (right).

1914-1915

1914-1915

1914-1915

1914-1915

1914-1915

1914-1915

# Physical Chemistry

Groupleader: Prof.dr. G. Frens  
Addres: Delft University of Technology  
Faculty of Chemical Technology and Materials  
Science  
Julianalaan 136  
NL 2628 BL Delft  
+31-15-278 5180  
G.Frens@STM.TUdelft.NL  
+31-15-278 4452



fax:



# Adsorption and pore penetration of polymers at anodized aluminium

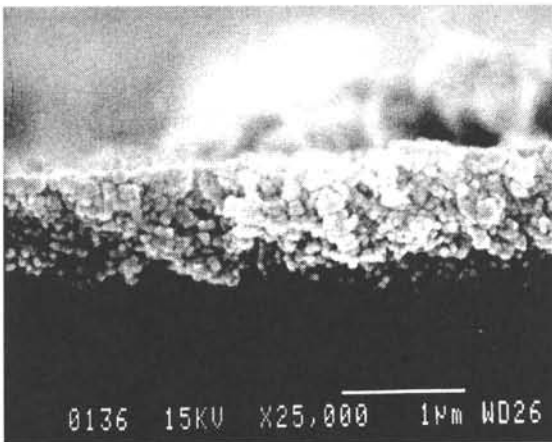
PhD student : S.G.O. de Haas ☎ 015-2787345 ✉ s.de haas@lr.tudelft.nl  
 Sponsor : IOP-Coatings/Adhesion Institute TUD



During the anodic pretreatment of aluminium, a porous oxide layer is formed. Ageing of this layer, before applying a coating, reduces the adhesion quality.

E. Margarita observed that ageing of the aluminium results in a lower surface energy ('activity') and a different aluminium oxide structure (see elsewhere in this book).

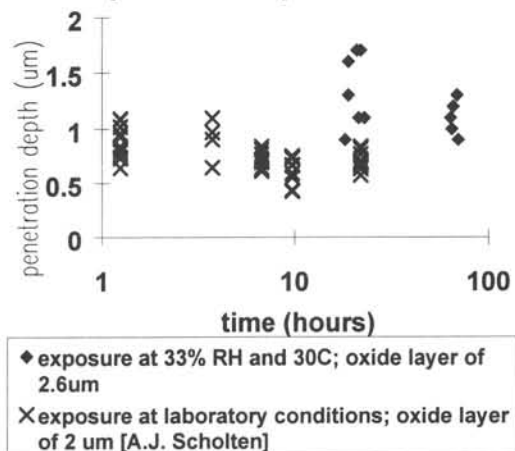
A lower surface activity is expected to decrease the polymer adsorption and the pore penetration on this surface. Polymer adsorption involves a loss of entropy caused by a less favorable polymer conformation. Interaction of the polymer with the activated aluminium surface involves an energy gain which has to compensate for the entropy loss for adsorption to occur.



A polyvinylchloride/vinylacetate (87/13) melt is pressed against aluminium of different exposure times after pretreatment. Subsequently, the aluminium and the oxide are dissolved. Contact angle measurements on the polymer plate enable us to calculate the surface energy which is a measure of adsorption. SEM fractography is used for measuring the polymer penetration depth into pores of the oxide layer (see photo).

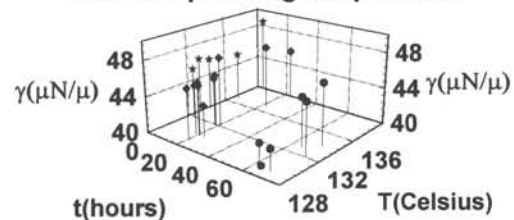
As we can see in figure 1 the polymer penetration decreases with an increasing exposure time of the bare substrate.

**figure 1: polymer penetration depth versus exposure time**



There also seems to be a lower surface tension for a longer exposure time and at lower pressing temperatures (figure 2).

**figure 2: surface tension versus exposure time and pressing temperature**



At the moment we are working on the reduction of the spreading in order to confirm these results and identify the parameters for optimal adhesion on aluminium.

[1] A.-J. Scholten, Report, Delft University of Technology, Faculty of Chemical Technology and Material Science, July 1996.



THE UNIVERSITY OF CHICAGO  
LIBRARY

1962

1963

1964

1965

1966

1967

1968

# Adsorption and Oxidation of Formaldehyde on Various Metals

Marnix ten Kortenaar<sup>1,2</sup>, Gert Frens<sup>1</sup>, Zvonimir Kolar<sup>2</sup>, Jeroen de Goeij<sup>2</sup>

<sup>1)</sup> *Sektie Fysische Chemie, Faculteit STM*

<sup>2)</sup> *Sektie Radiochemie, Interfacultair Reactor Instituut*

Sponsor: NWO/SON

Tel.: +31-15-2781485

E-mail: Kortenaar@iri.tudelft.nl

## Introduction

Electroless plating is a process in which metals may be deposited on a substrate by a suitable reducing agent. Applications of it for the filling of contact holes of VLSI structures depend on the kinetic control of the deposition process. The rate of exchange and oxidation of formaldehyde may rule the rate of metal deposition and is studied by both radiochemical and electrochemical methods.

## Methods and Results

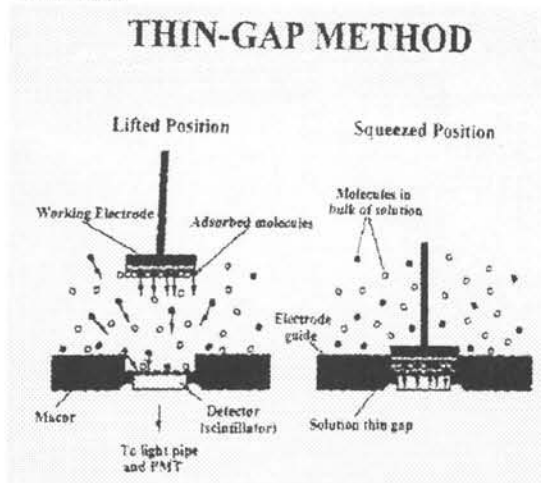
The rate of adsorption and exchange of formaldehyde is studied on various metals by pressing a flat electrode with adsorbed radioactive-labeled formaldehyde molecules onto a glass scintillator. A PMT detects converted signals, and fractional surface coverages are readily obtained by subtracting 'background' signals, counted when no adsorption occurs (Figure 1).

Adsorption is studied as a function of time, pH, concentration, temperature and potential and first measurements have shown that exchange of formaldehyde on silver is a

rapid process, likely being dependent on the potential applied and a range of system parameters.

In addition, the rate of exchange and oxidation of formaldehyde on gold and silver has been studied by voltammetry, mass spectrometry and AC impedance spectroscopy. Fitting of the results is currently being done by equivalent-circuit analysis, transfer function procedures and compartmental analysis. The various complementary fitting procedures will yield the rate constants of the exchange and oxidation processes.

**Fig.1.** Qualitative illustration of thin-gap method.



Received of the Treasurer of the County of ...  
the sum of ... Dollars ...  
for ...

...  
...

...

...

...

...

...

...

...

...

...

...

...

...

...



# IMPROVEMENT OF COHESIVE AND ADHESIVE PROPERTIES OF WHEY PROTEINS

AIO : A.A.C.M. Rutten

☎ : 015-278 61 81

✉ : a.rutten@stm.tudelft.nl

Sponsor : IOP Industrial Proteins

Borculo Whey Products

National Starch & Chemical BV

## Introduction

It is expected that on a short term the supply of whey proteins at the world market will increase. Therefore, it is essential to develop new applications of whey proteins. Non-food applications are preferred, because there is no competition with other proteins, but with synthetic polymers. Very interesting fields of application are adhesives and coating/films. The aim of this project is to gain knowledge about the adhesive and cohesive properties of whey proteins and their performance in this respect.

## Description of the project

In this project the emphasis will be on  $\beta$ -lactoglobulin because it is the most abundant protein in whey and much is known about its structure, which greatly facilitates the interpretation of the results in structural terms. In a later stage of the project other proteins and lactose will be included.

For a strong adhesion between protein and substrate the distance dependent Van der Waals attraction has to be strong, which requires adsorption of the protein molecules in a sufficiently flat conformation. Therefore, the globular  $\beta$ -lactoglobulin molecules have to be (partly) unfolded, which we will realize by heating and by the use of certain organic solvents, water miscible or not.

The natural tendency towards depletion of these unfolded molecules has to be compensated by polar interactions of functional groups in the protein chain with the substrate. These functional groups may be already present in the protein chain and become available by the unfolding process, or they may be introduced or amplified by modification.

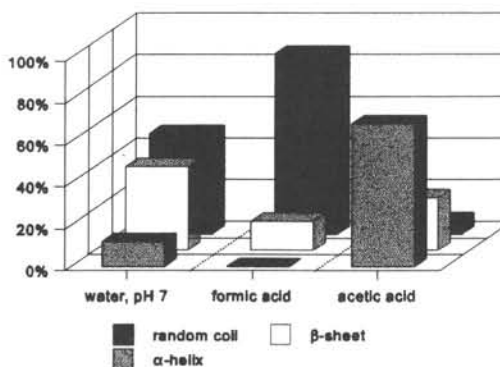
Functional properties, such as adsorption

behavior, film forming, adhesive strength and mechanical properties of the films, will be studied, as well as the degree of denaturation, hydrophobicity and the aggregation behavior. These properties will be related to the polarity of both solvent and substrate.

## Experimental

Globular proteins contain a certain amount of ordered structure, like  $\alpha$ -helices and  $\beta$ -sheets. These structures can be broken by organic solvents. We have used circular dichroism spectroscopy to determine the secondary structure of  $\beta$ -lactoglobulin in water at different pH-values and in several organic solvents. A few of these results are represented in the figure below.

We will try to relate the (in)stability of the protein to the solvents characteristics, like relative permittivity, dipole moment, electron donor and acceptor ability etc. But more important, we will try to find the relation between the secondary and tertiary structure of the protein and its ability to adsorb on a certain surface and the strength of this adsorption.



# THE HISTORY OF THE UNITED STATES OF AMERICA

FROM THE FIRST SETTLEMENTS TO THE PRESENT TIME

BY JAMES M. SMITH

The history of the United States of America is a story of growth and development. It begins with the first settlers who came to the shores of the New World, seeking a new life and a new land. They found a land of great beauty and potential, but also a land of great challenges. The early years were marked by struggle and hardship, but the spirit of the settlers was one of determination and courage. They built a nation that would become a model for the world.

The story of the United States is a story of the people who have lived on its soil. It is a story of the men and women who have shaped the nation, from the first settlers to the present day. It is a story of the values and ideals that have guided the nation, from the pursuit of freedom and justice to the pursuit of the American dream. The history of the United States is a story of the people who have made it what it is today.

The history of the United States is a story of the people who have lived on its soil. It is a story of the men and women who have shaped the nation, from the first settlers to the present day. It is a story of the values and ideals that have guided the nation, from the pursuit of freedom and justice to the pursuit of the American dream. The history of the United States is a story of the people who have made it what it is today.

The history of the United States is a story of the people who have lived on its soil. It is a story of the men and women who have shaped the nation, from the first settlers to the present day. It is a story of the values and ideals that have guided the nation, from the pursuit of freedom and justice to the pursuit of the American dream. The history of the United States is a story of the people who have made it what it is today.

The history of the United States is a story of the people who have lived on its soil. It is a story of the men and women who have shaped the nation, from the first settlers to the present day. It is a story of the values and ideals that have guided the nation, from the pursuit of freedom and justice to the pursuit of the American dream. The history of the United States is a story of the people who have made it what it is today.

The history of the United States is a story of the people who have lived on its soil. It is a story of the men and women who have shaped the nation, from the first settlers to the present day. It is a story of the values and ideals that have guided the nation, from the pursuit of freedom and justice to the pursuit of the American dream. The history of the United States is a story of the people who have made it what it is today.

# EFFECTIVITY OF DETERGENTS IN DYNAMIC SURFACE CLEANING

**A. Timmerman and G. Frens**  
*Laboratory for Physical Chemistry*  
*Delft University of Technology*  
*Delft, The Netherlands*

Sponsor: IR-TNO

Tel: +31-152782638  
email: A.Timmerman@stm.tudelft.nl

## *Introduction*

The washing of textile can be characterized empirically by the 'Sinner-factors': energy, temperature, chemistry and time. Departing from these factors the washing process can be optimized. If, however, the backgrounds of the Sinner factors are known, it will be possible to optimize the washing process from a more fundamental point of view. From earlier research it was concluded that a soiled textile could never be cleaned in a normal washing process if the most important mechanism governing the mass transfer from fabric to detergent solution were diffusion. Therefore, in this research it is supposed that there is a flow both along the fabric-surfactant solution interface and in the fabric yarns.

## *Theory*

At high surfactant concentrations a surfactant bilayer is formed between the flowing liquid and the surface of the hydrophilic yarn. During the washing process fabrics are moved and deformed continuously. By stretching the fabric, liquid (the surfactant solution) is squeezed from pores in the yarns. This makes the second surfactant layer flow along the fabric-liquid interface. This flow along the interface may be advantageous for the

effectivity of the washing process by causing local supersaturation in the bilayer, which gives rise to instabilities. These instabilities can cause a motion perpendicular to the textile surface.

## *Experimental*

It is envisaged that under certain temperature and pH conditions highly concentrated solutions (about 3 times the critical micelle concentration) can form bilayers at a hydrophilic surface of a capillary. If concentrated surfactant solutions will flow more quickly through this capillary than diluted solutions, this indicates a slip condition at the wall of the capillary. In order to find evidence for flow along the liquid-fabric interface, surfactant solutions of different concentrations are pushed through narrow glass capillaries of different lengths and diameters. The flow through the capillary is measured as a function of hydrostatic pressure. If non-linear effects in the pressure-flow curve are a function of concentration, instabilities at the fluid textile interface are present. At standard conditions (pH = 7, T=22°C) no obvious non-linear effects are found for SDS solutions up to 7 times the cmc. Future measurements are planned at higher temperature and pH values.



# Materials Physics

Substitute Groupleader: Dr. B.J. Thijsse  
Addres: Delft University of Technology  
Faculty of Chemical Technology and Materials  
Science  
Rotterdamseweg 137  
NL 2628 AL Delft  
+31-15-278 2221  
B.J.Thijsse@STM.TUdelft.NL  
+31-15-278 6730



fax:



# Defects in thin films produced by ion-beam assisted deposition

*Jan van der Kuur, Jacqueline van der Linden, Martin Pols, Bas Korevaar, Peter Klaver, and Barend Thijsse*

*Materials Physics Division, Department of Chemistry and Materials Science  
Delft University of Technology*

Sponsors: FOM, DUT

Tel: +31 15 278 4922

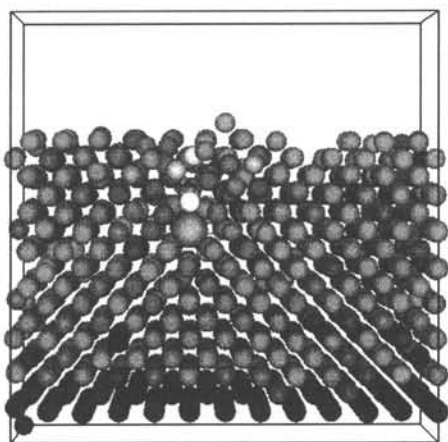
E-mail: J.vanderkuur@stm.tudelft.nl

The goal of this project is to understand the initial growth process of thin solid state films and the origins and properties of defects in the surface and near-surface regions. In addition we want to quantify on an atomic level the effects of concurrently impacting low-energy noble gas ions during the growth. This technique is called ion-beam assisted deposition.

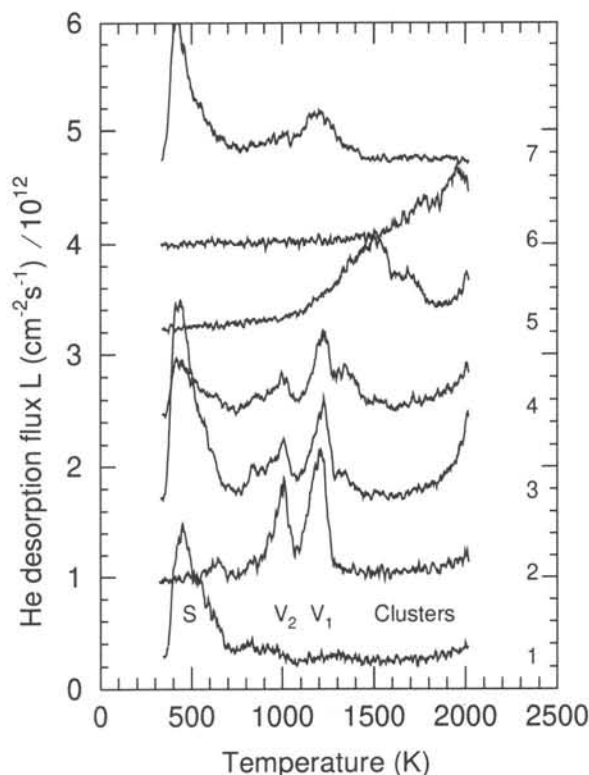
The significance of ion assistance during film growth is the controlled deposition of kinetic energy. This leads to various nanometer- and micrometer-scale defect phenomena which are interesting both from a fundamental and from an applied viewpoint.

The defect state of the film is measured by bringing small ions ( $\text{He}^+$ ) into the film. Acting as atomic-scale diffusing probes, some ions (which have become atoms) will be trapped by defects. If the sample temperature is then increased, the trapped atoms dissociate from the defects, desorb from the film, and are mass-detected in a UHV-system. Information about the defect state of the film is contained in the desorption signal as a function of temperature.

In 1996 we have extensively studied Mo films deposited with and without  $\text{Ar}^+$  assistance, both experimentally and by Molecular Dynamics computer simulations. Two figures illustrate in condensed form some of the potential of the current methods.



Mo film shortly after the impact of a 250 eV  $\text{Ar}^+$  ion (large sphere). Greyscale indicates kinetic energy. The temporary disorder along the entrance path is clearly seen. This impact causes a 6-atom replacement collision leading up to the creation of a Mo adatom and substitutional trapping of the  $\text{Ar}^+$  ion. In other simulations the ion was found to create additional vacancies and vacancy clusters, in agreement with the experimental results.



(1) He desorbing from a deposited 5 Å Mo film, indicating weak traps just below the surface (desorption peak S).

(2) Same spectrum as (1) but film was first covered by a 5 Å overlayer before desorption: the coverage has fully transformed the surface traps into normal vacancies (peaks  $V_2$  and  $V_1$ ).

(3) Same as (1) but film is 50 Å thick. (4) Same as (3) but film was first covered by a 20 Å overlayer: even an overlayer this thick can not fully cover the 50 Å film (the S peak is still visible), indicating a rougher surface of the 50 Å film than that of the 5 Å film.

(5) Same as (4) but overlayer was grown with  $\text{Ar}^+$  assistance: in the overlayer vacancy clusters are produced in which He from the base layer is trapped before final desorption (peaks above 1300 K).

(6) Same as (4) but overlayer thickness is 500 Å: films this thick (no  $\text{Ar}^+$  assistance) contain large vacancy clusters in which He from the base layer is trapped before final desorption (peak at 1900 K).

(7) Same film as (6) but He was implanted into the top 30 Å of the film after deposition, instead of into the 50 Å base layer under it before deposition. The spectrum shows that the vacancy clusters mentioned under (6) are not located in the top part of the film.





# Physical and Chemical Materials Science

Group leader: Prof.dr.ir. E.J. Mittemeijer  
Address: Delft University of Technology  
Faculty of Chemical Technology and Materials  
Science  
Rotterdamseweg 137  
NL 2628 AL Delft  
+31-15-278 2207  
E.J.Mittemeijer@STM.TUdelft.NL  
+31-15-278 6730



fax:



# On the initial oxidation of iron: quantification of growth kinetics

P.C.J. Graat, M.A.J. Somers and E.J. Mittemeijer

Physical Chemistry of the Solid State

Phone: +31 15 278 2260

Sponsor: Delft University of Technology

E-mail: p.graat@stm.tudelft.nl

## Introduction

Knowledge of metal oxidation is important for understanding catalysis and corrosion. The most-comprehensive model for initial oxide-film growth on metals is due to Fromhold & Cook<sup>1</sup>. So far, this model was hardly applied to experimental data. This work<sup>2</sup> provides new data on the initial oxidation kinetics of pure iron and attempts to interpret the results in terms of the Fromhold-Cook model.

## Experimental

Polycrystalline iron was, after sputter cleaning with 1.0 kV Ar<sup>+</sup> ions and annealing at 700 K, oxidised at  $p_{O_2}=10^{-4}$  Pa and at temperatures ranging from 300 K to 500 K. Ellipsometry was used for monitoring the oxide-film thickness as a function of time.

## Results

The experimental curves in Fig. 1 show the typical shape for initial oxidation of metals.

To model these data, the most sensitive parameters in the Fromhold-Cook model, i.e. the energy barrier for cation diffusion,  $W$ , and the work functions,  $\chi_0$  and  $\chi_L$  at the metal-oxide and oxide-oxygen interface, respectively, were taken as fit parameters. This results in the dotted lines in Fig.1.

Evidently, the assumption of stationary values for  $W$ ,  $\chi_0$  and  $\chi_L$  during oxidation is not realistic. Particularly  $\chi_L$  is likely to change during oxide-film growth, due to a change of the surface oxygen content. Accordingly, the model was fitted with a time-dependent  $\chi_L$ . The

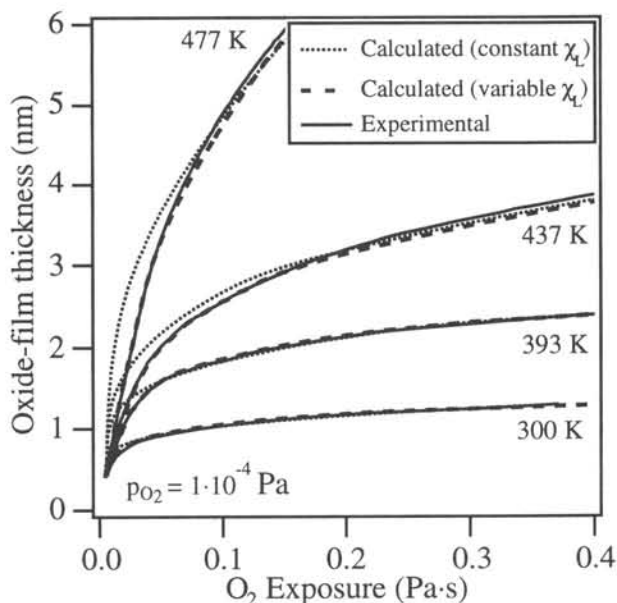


FIG. 1 Experimental and calculated oxide film thickness versus  $O_2$  exposure at the indicated temperatures.

curves thus obtained are represented by the dashed lines in Fig. 1. The experimental and theoretical (dashed) curves agree very well for thickness values below 3 nm. The critical value of 3 nm corresponds to the thickness where thermal emission governs electron transport rather than electron tunnelling<sup>1,2</sup>.

The calculated change of  $\chi_L$  during oxidation<sup>2</sup> agrees qualitatively with published results on the change of the work function observed during oxidation of metals.

## References

1. A.T. Fromhold, Jr., Theory of Metal Oxidation; Volume I (North-Holland, Amsterdam, 1976).
2. P.C.J. Graat, M.A.J. Somers, A.M. Vredenberg and E.J. Mittemeijer, J. Appl. Phys, accepted for publ.



# Low-*T* dry oxidation on pure aluminium crystal grain surfaces as observed with photoelectron and auger electron spectroscopy

L.P.H. Jeurgens, W.G. Sloof, F.D. Tichelaar, C.G. Borsboom and E.J. Mittemeijer

Section Physical Chemistry of the Solid State

Sponsors: NWO/FOM

Tel: +31-15-278 8397

E-mail: Jeurgens@stm.tudelft.nl

## Introduction

This research project focuses on the initial stages of oxidation as well as on later stages of oxide growth of aluminium. In particular, the role of alloying elements on the oxidation mechanism, growth kinetics, and oxide structure, will be investigated. The final goal is to arrive at models describing the growth kinetics in relation to the developing microstructure both in the metal substrate and the oxide layer, and test its validity on the oxidation of Al-Mg and Al-Si alloys.

## Experimental

Oxidation experiments were performed on a clean Al(110) and Al(112) crystal grain surface as a function of total oxygen exposure  $Q$  at a constant oxygen pressure of  $1 \times 10^{-6}$  Torr and an oxidation temperature of 300 K and 673 K, resp. Each oxide layer grown was studied with XPS. The oxide growth kinetics were investigated by observing the change in oxide-film thickness  $d$  with increasing total oxygen exposure. Changes in the chemical state of Al as a function of substrate orientation,  $d$ ,  $T$ ,  $P(O_2)$  and oxidation time are studied in a Chemical State plot. This plot, as presented in Figure 1, is obtained by plotting the Al  $KL_{23}L_{23}$  Auger kinetic energies  $E_K$  of the oxidic  $KL_{23}L_{23}$  peak component on the ordinate and the corresponding Al 2*p* binding energy  $E_B$  of the oxidic 2*p* peak component, in reverse, on the abscissa. The metallic and oxidic peak components were resolved from the measured peak envelop by a fit procedure. In Fig.1, the Modified Auger Parameter  $\alpha' = E_K(KL_{23}L_{23}) + E_B(2p)$ , which is independent upon charging, lies along axes with slope +1.

## Discussion

At  $T=305$  K and  $Q=500$  L, oxide growth is completed and a 0.25 nm thick oxide film has formed on both faces. At  $T=673$  K and  $Q=1000$  L, an oxide film of 2.0 and 2.5 nm has formed on the Al(110) and Al(112) face, respectively, and

up to this point a significant decrease in oxidation rate is not yet observed. Moreover, at  $T=673$  K, initial oxide growth proceeds much faster on the relative more open Al(112) than on the more rigid Al(110) face.

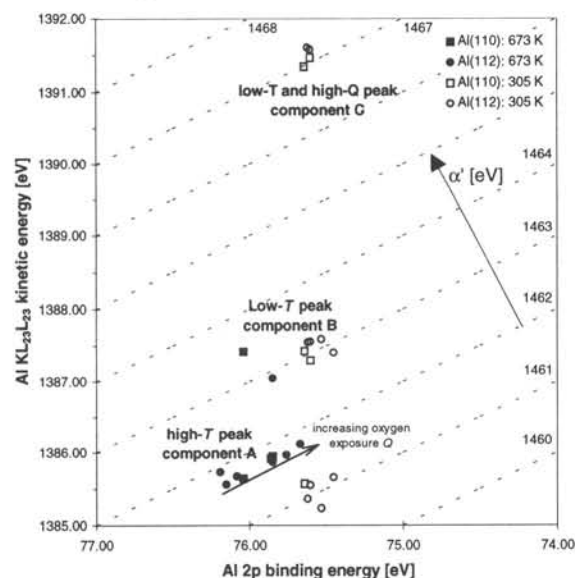


**Figure 1:** Chemical state plot of Al-oxides grown on a pure Al(110) and Al(112) substrate at  $T=305$  K and  $T=673$  K by exposure to pure  $O_2(g)$ .

If Al in the oxide layer is present in more than one chemical state as a result of e.g. a different surrounding of oxygen atoms, then an Auger fine structure is expected. This is reflected in Fig.1 by the difference in  $\alpha'$  found between the three different  $KL_{23}L_{23}$  oxidic peak components A, B and C. The relative peak intensity of each of these oxidic components is found to be strongly dependent upon  $T$ . Our next step will be to relate these possible different oxide phases with the crystallographic structure of the oxide layer as resolved in a HRTEM-cross section. A decrease in Al 2*p* binding energy of the oxidic peak component A with increasing total oxygen exposure is observed for  $T=673$  K (See: Fig.1). This trend possibly indicates a decrease in ionicity of the Al-O bond with increasing oxide-film thickness as a result of a change in valence charge density around the Al nucleus.

1. The first part of the document discusses the importance of maintaining accurate records of all transactions and activities. It emphasizes that proper record-keeping is essential for transparency and accountability, particularly in financial matters. The text suggests that organizations should implement robust systems to track every aspect of their operations, from procurement to sales.

2. The second section focuses on the role of technology in modern business management. It highlights how digital tools can streamline processes, reduce errors, and improve overall efficiency. The author argues that embracing technology is not just a competitive advantage but a necessity for long-term success in today's fast-paced market.

3. The third part of the document addresses the challenges of human resource management. It discusses the importance of attracting and retaining top talent, as well as the need for continuous training and development. The text suggests that organizations should create a supportive work environment that encourages innovation and collaboration among employees.

4. The fourth section explores the impact of market trends and external factors on business performance. It notes that companies must remain vigilant and adaptable to changes in the market, such as shifts in consumer behavior or new regulatory requirements. The author advises that strategic planning and risk management are crucial for navigating these uncertainties.

5. The final part of the document provides a summary of the key points discussed and offers some concluding thoughts. It reiterates the importance of a holistic approach to business management, where all aspects of the organization are aligned towards common goals. The text ends with a call to action, encouraging readers to implement the strategies discussed and strive for excellence in their respective fields.

# A model for stress in thin layers induced by misfitting particles An origin for growth stress

*J.-D. Kamminga, Th.H. de Keijser, R. Delhez and E.J. Mittemeijer*  
Section Physical Chemistry of the Solid State

Sponsor: IOP Oppervlaktetechnologie

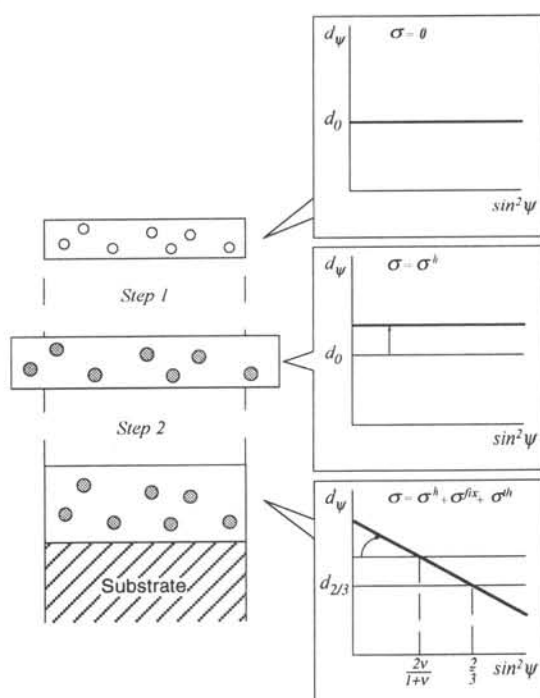
Tel: +31-15-2782251

E-mail: Kamminga@stm.tudelft.nl

A model has been developed to describe the state of stress in thin layers, induced by misfitting particles.

## Model

A freestanding, hole containing layer with lateral dimensions equal to those of the substrate is considered.



**Step 1:** Misfitting particles are introduced into the holes leading to:

- Isotropic expansion
- Hydrostatic stress  $\sigma^h$

**Step 2:** Layer is matched to the substrate by  $\sigma^{fix}$ . Cooling down yields thermal stress  $\sigma^{th}$ .

- Planar stresses  $\sigma^{fix}$ ,  $\sigma^{th}$

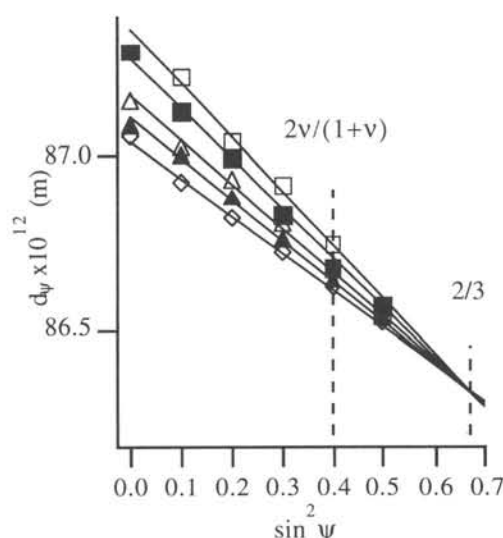
From the model it follows that  $\sigma^{fix} = -1.5 \cdot \sigma^h$  and that  $d_{2/3}$  ( $d_\psi$  at  $\sin^2 \psi = 2/3$ ) does not depend on growth stress ( $\sigma^h$ ,  $\sigma^{fix}$ ).

Consequently  $\sin^2 \psi$  plots of a series of layers, having equal  $\sigma^{th}$  but different growth stresses, should intersect at  $d_{2/3}$ .

## Experimental illustration

TiN layers of various thicknesses were magnetron sputtered onto tool steel at 620 K, leading to a  $\sigma^{th}$  of about -1.5 GPa. X-ray diffraction measurements revealed additional growth stresses of -2 to -6 GPa, believed to be caused by interstitial atoms.

A point of intersection for  $\sin^2 \psi$  plots at  $d_{2/3}$  is expected.



$\sin^2 \psi$  plots for TiN layers. 422 reflections were used. Fits (full lines) were forced to intersect at  $\sin^2 \psi = 2/3$ .

## Conclusion

Predictions of the model clearly coincide with the results of X-ray diffraction stress measurements for magnetron sputtered TiN layers.

## X-ray diffraction stress measurements

The lattice spacings  $d_\psi$  of lattice planes HKL making an angle  $\psi$  with the specimen surface, are plotted versus  $\sin^2 \psi$ . The planar stress in the layer follows from the slope of a linear fit through the data points.

Actions of  $\sigma^h$  and  $\sigma^{fix}$ ,  $\sigma^{th}$ :

- $\sigma^h$ : Vertical shift
- $\sigma^{fix}$ ,  $\sigma^{th}$ : Rotation at  $\sin^2 \psi = 2v/(1+v)$

1913 Jan 10

Received of Mr. J. H. ...  
the sum of ...  
for ...

1913 Jan 11  
Received of Mr. J. H. ...  
the sum of ...  
for ...

1913 Jan 12  
Received of Mr. J. H. ...  
the sum of ...  
for ...

1913 Jan 13  
Received of Mr. J. H. ...  
the sum of ...  
for ...

1913 Jan 14  
Received of Mr. J. H. ...  
the sum of ...  
for ...

1913 Jan 15  
Received of Mr. J. H. ...  
the sum of ...  
for ...

1913 Jan 16  
Received of Mr. J. H. ...  
the sum of ...  
for ...

1913 Jan 17  
Received of Mr. J. H. ...  
the sum of ...  
for ...



## Quasi in situ sequential sulphidation of CoMo/Al<sub>2</sub>O<sub>3</sub> studied using High Resolution Electron Microscopy.

P.J. Kooyman<sup>1</sup>, J.G. Buglass<sup>2</sup>, H.R. Reinhoudt<sup>3</sup>, A.D. van Langeveld<sup>3</sup>, H.W. Zandbergen<sup>1</sup> and J.A.R. van Veen<sup>2</sup>.

1) National Centre for High Resolution Electron Microscopy, Rotterdamseweg 137, 2628 AL Delft, The Netherlands.

2) SRTCA, P.O.Box 38000, 1030 BN Amsterdam, The Netherlands.

3) Faculty of Chemical Technology and Materials Science, Delft University of Technology, Julianalaan 136, 2628 BL Delft, The Netherlands.

### INTRODUCTION

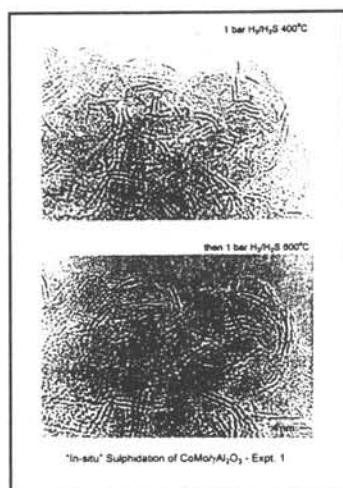
The sulphidation process can best be studied by examining exactly the same areas of a sample after sequential sulphidation steps. The formation and growth of the active phase can be followed by examining a sample after subsequent sulphidation steps without exposure to air during transport to and from the microscope and the sulphidation set-up.

### EXPERIMENTAL

HREM was performed using a Philips CM30ST-FEG at 300 kV.

Sequential sulphidation was performed by sulphiding the sample holder containing the sample without exposure to air by transfer to and from the microscope via a specially developed vacuum transfer system.

### RESULTS



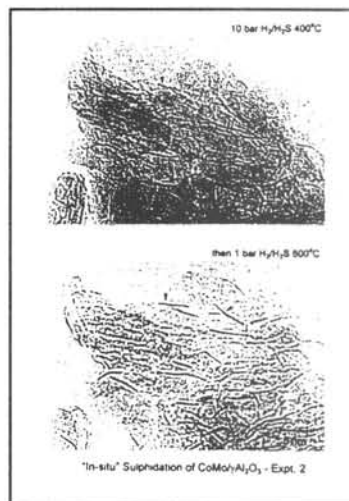
Thiophene HDS 350C 6vol%/H<sub>2</sub>  
conversion to C4 products

28.4 %

40.2 %

20.5 %

23.7 %



### CONCLUSIONS

- \* 10 bar 1st step yields more stacking than 1 bar 1st step
- \* 2nd sulphidation step increases the length of the slabs
- \* 2nd sulphidation step decreases thiophene HDS performance
- \* 10 bar 400C 1st step then 1 bar 600C 2nd step leads to increased crystallinity and dramatically decreased catalytic performance
- \* A defect slab structure is the active phase?

THE UNIVERSITY OF CHICAGO

THE UNIVERSITY OF CHICAGO

THE UNIVERSITY OF CHICAGO

THE UNIVERSITY OF CHICAGO

THE UNIVERSITY OF CHICAGO

THE UNIVERSITY OF CHICAGO

THE UNIVERSITY OF CHICAGO

THE UNIVERSITY OF CHICAGO

THE UNIVERSITY OF CHICAGO

THE UNIVERSITY OF CHICAGO

THE UNIVERSITY OF CHICAGO

THE UNIVERSITY OF CHICAGO

THE UNIVERSITY OF CHICAGO

# Growth and annealing of Ag-Ni layers - stresses and twin densities

L. Velterop<sup>+</sup>, R. Delhez<sup>+</sup>, Th.H. de Keijser<sup>+</sup>, E.J. Mittemeijer<sup>+</sup>, D. Reefman<sup>\*</sup>

<sup>+</sup>Section Physical Chemistry of the Solid State

<sup>\*</sup>Philips (sponsor)

Tel: + 31-15-2786785

e-mail: L.Velterop@stm.tudelft.nl

## Introduction

Thin sputtered layers can contain much higher stresses and twin densities than bulk materials, due to the non-equilibrium conditions during deposition. It is known that impurities can enhance the formation of twins. Using TEM and XRD, the influence of a second element on the stress and the twin density in the layers is examined [1].

## Samples

Thin Ag-Ni layers (0.5  $\mu\text{m}$  thick with 0, 14.7, 21.6 and 28.0 at.% Ni) were sputtered onto Si single crystal substrates. It was found that Ag and Ni in the as-prepared layers formed an (almost homogeneous) solid solution.

## Stress and twin density determination

The stress can be obtained from the XRD lattice parameter as a function of  $\psi$ , the angle between the actually diffracting lattice planes and the layer surface ( $\sin^2\psi$  method).

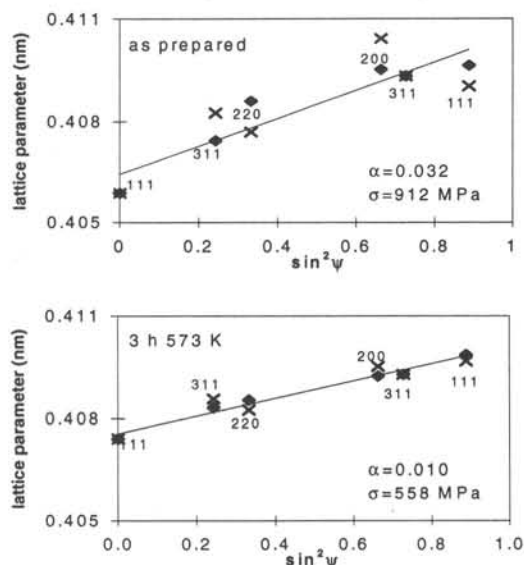


**Fig.1:** As measured (x) and corrected (♦) lattice parameter versus  $\sin^2\psi$  of the as prepared sample (15 at.% Ni) and after 3 h annealing at 573 K.  $\alpha$  = twin probability.

The lattice parameter- $\sin^2\psi$  plot exhibits in general a straight line, the slope of which is a measure for the stress. Deviations from this linear behaviour can occur due to the presence of twins. Twins introduce a peak shift, the magnitude of which is dependent on the twin density and the orientation of the diffracting lattice planes {HKL} with respect to the twin plane.

In the present case, the  $\sin^2\psi$  plots show large, systematic deviations from a straight line (fig.1), although a linear relation is expected due to the {111} texture present [1]. These deviations increase with increasing Ni content and decrease with increasing annealing time. The twin density and the stress were determined by a fitting procedure in which a twin density was refined such that a shift of the data points towards a best straight line was obtained (see fig. 1). The twin densities determined this way are comparable with the values estimated from TEM images.

## Results

Pure Ag layers contain no twins and Ag-Ni layers have a high density of twins. This twin density increases with increasing Ni content. Upon annealing spherical Ni-rich precipitates (crystallographically oriented parallel to the Ag-rich matrix) are formed and the twin density decreases.

The calculated stresses are very high in the as prepared Ag-Ni layers (almost 1 GPa) and almost zero for pure Ag. Upon the precipitation of the Ni, the stresses decrease.

## Conclusion

In sputtered Ag-Ni layers Ni is dissolved in Ag; it enhances twin formation and enables Ag to sustain high stresses.

[1]L. Velterop et al. Mat. Res. Soc. Proc. **472** (1997)

ORIGINAL ARTICLES

1. The Effect of the Diet on the Blood Sugar in the Normal Individual and in the Diabetic Individual. (Continued from page 1000.)

2. The Effect of the Diet on the Blood Sugar in the Normal Individual and in the Diabetic Individual. (Continued from page 1000.)

3. The Effect of the Diet on the Blood Sugar in the Normal Individual and in the Diabetic Individual. (Continued from page 1000.)

4. The Effect of the Diet on the Blood Sugar in the Normal Individual and in the Diabetic Individual. (Continued from page 1000.)

5. The Effect of the Diet on the Blood Sugar in the Normal Individual and in the Diabetic Individual. (Continued from page 1000.)

6. The Effect of the Diet on the Blood Sugar in the Normal Individual and in the Diabetic Individual. (Continued from page 1000.)

7. The Effect of the Diet on the Blood Sugar in the Normal Individual and in the Diabetic Individual. (Continued from page 1000.)

8. The Effect of the Diet on the Blood Sugar in the Normal Individual and in the Diabetic Individual. (Continued from page 1000.)

9. The Effect of the Diet on the Blood Sugar in the Normal Individual and in the Diabetic Individual. (Continued from page 1000.)

10. The Effect of the Diet on the Blood Sugar in the Normal Individual and in the Diabetic Individual. (Continued from page 1000.)

11. The Effect of the Diet on the Blood Sugar in the Normal Individual and in the Diabetic Individual. (Continued from page 1000.)

12. The Effect of the Diet on the Blood Sugar in the Normal Individual and in the Diabetic Individual. (Continued from page 1000.)

13. The Effect of the Diet on the Blood Sugar in the Normal Individual and in the Diabetic Individual. (Continued from page 1000.)

14. The Effect of the Diet on the Blood Sugar in the Normal Individual and in the Diabetic Individual. (Continued from page 1000.)

15. The Effect of the Diet on the Blood Sugar in the Normal Individual and in the Diabetic Individual. (Continued from page 1000.)

16. The Effect of the Diet on the Blood Sugar in the Normal Individual and in the Diabetic Individual. (Continued from page 1000.)

17. The Effect of the Diet on the Blood Sugar in the Normal Individual and in the Diabetic Individual. (Continued from page 1000.)

18. The Effect of the Diet on the Blood Sugar in the Normal Individual and in the Diabetic Individual. (Continued from page 1000.)

19. The Effect of the Diet on the Blood Sugar in the Normal Individual and in the Diabetic Individual. (Continued from page 1000.)

20. The Effect of the Diet on the Blood Sugar in the Normal Individual and in the Diabetic Individual. (Continued from page 1000.)

21. The Effect of the Diet on the Blood Sugar in the Normal Individual and in the Diabetic Individual. (Continued from page 1000.)

22. The Effect of the Diet on the Blood Sugar in the Normal Individual and in the Diabetic Individual. (Continued from page 1000.)

# Corrosion Technology and Electrochemistry

Groupleader: Prof.dr. J.H.W. de Wit  
Addres: Delft University of Technology  
Faculty of Chemical Technology and Materials  
Science  
Rotterdamseweg 137  
NL 2628 AL Delft  
+31-15-278 2196  
J.H.W.deWit@STM.TUdelft.NL  
+31-15-278 6730

  
  
fax:

# THE HISTORY OF THE CITY OF BOSTON

BY  
JOHN H. COOK,  
OF THE  
CITY OF BOSTON.  
PUBLISHED BY  
J. B. LEECH, 1854.

# CORROSION PROTECTION OF STEEL IN MOLTEN CARBONATES BY CERAMIC COATINGS

M. Keijzer<sup>a,b</sup>, P. J. J. M. van der Put<sup>a</sup>, K. Hemmes<sup>b</sup>, J. H. W. de Wit<sup>b</sup>, and J. Schoonman<sup>a</sup>

<sup>a</sup> Delft University of Technology, Laboratory for Applied Inorganic Chemistry, Julianalaan 136, 2628 BL Delft, The Netherlands

<sup>b</sup> Delft University of Technology, Laboratory for Corrosion Technology, Electrochemistry, and Spectroscopy, Rotterdamseweg 137, 2628 AL Delft, The Netherlands

Tel.: +31-15-278 2637

E-mail: m.keijzer@stm.tudelft.nl

## Introduction

Corrosion is a major lifetime-limiting factor in molten carbonate fuel cells (MCFCs). Cell components subject to corrosion are the separator plates and the current collectors, which are both made of stainless steel or nickel alloys. Our goal is to protect steel components against corrosion by a ceramic coating. In a previous study<sup>1</sup>, we selected TiN, TiC and Ce-based ceramics as suitable coating materials because of their high electronic conductivity and corrosion resistance in preliminary exposure tests with molten carbonates.

## Experimental

Stainless steel 304 substrates were coated with a dense TiN layer by thermally activated chemical vapour deposition (CVD). The corrosion of these TiN-coated samples was tested electrochemically in a MCFC environment, a melt of 62/38 molar%  $\text{Li}_2\text{CO}_3/\text{K}_2\text{CO}_3$  at 650°C under MCFC-cathode gas or MCFC-anode gas.

## Results and discussion

Corrosion layer thickness on samples was determined from cross-sections with light microscopy. After 30 days of exposure under anode gas, a corrosion layer of about 2  $\mu\text{m}$  was visible on the original coating. After 30 days of exposure under cathode gas, three corrosion layers were visible of about 20  $\mu\text{m}$  in total as shown in Fig. 1.

The corrosion layer thickness on steel was comparable after only one day of exposure.

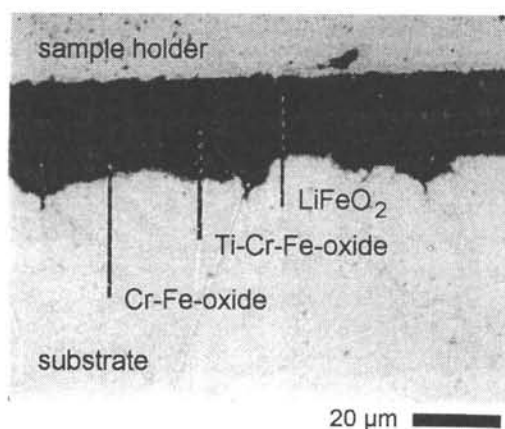


**Fig. 1** Light microscopy cross-section of TiN-coated steel after 30 days of exposure under cathode gas

## Conclusions

The TiN-coating lowers corrosion in molten carbonates. Under cathode gas, the deposited layer is probably not lifetime protective, whereas under anode gas, the deposited layer might be suitable for corrosion reduction during long exposure times.

## Reference

1. M. Keijzer, K. Hemmes, P. J. J. M. van der Put, J. H. W. de Wit, and J. Schoonman, *Corrosion Sci.*, **39**, 183 (1997)

# THE HISTORY OF THE CITY OF BOSTON

As the city of Boston is one of the most important and interesting in the United States, it is not surprising that its history has been the subject of many works. The first of these was a small pamphlet by John Smith, published in 1630, which contained a brief account of the city's early history. This was followed by a number of other works, including a history by John Vane in 1630, and a more detailed history by John Vane in 1630.

The first of these works was a small pamphlet by John Smith, published in 1630, which contained a brief account of the city's early history. This was followed by a number of other works, including a history by John Vane in 1630, and a more detailed history by John Vane in 1630.

The first of these works was a small pamphlet by John Smith, published in 1630, which contained a brief account of the city's early history. This was followed by a number of other works, including a history by John Vane in 1630, and a more detailed history by John Vane in 1630.

The first of these works was a small pamphlet by John Smith, published in 1630, which contained a brief account of the city's early history. This was followed by a number of other works, including a history by John Vane in 1630, and a more detailed history by John Vane in 1630.

The first of these works was a small pamphlet by John Smith, published in 1630, which contained a brief account of the city's early history. This was followed by a number of other works, including a history by John Vane in 1630, and a more detailed history by John Vane in 1630.



# Electrochemical Impedance Measurements on Anodized Aluminium

*M.B.Spoelstra, D.H.van der Weijde, J.H.W.de Wit*

*Delft University of Technology, Laboratory for Materials Science and Engineering  
Rotterdamseweg 137, 2628 AL Delft, The Netherlands*

Sponsor: IOP Surface Technology (IOT 94007)  
E-mail: M.B.Spoelstra@stm.tudelft.nl

Tel: (+31)-15-2785081  
Fax: (+31)-15-2786730

## Introduction

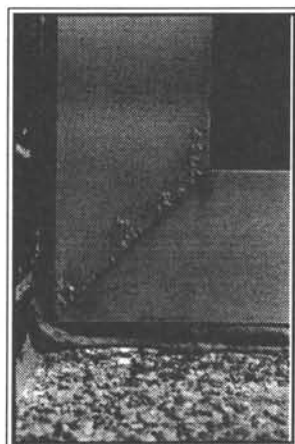


**Fig.1:** Filiform corrosion on an aluminium window frame

This picture shows an example of filiform corrosion; a problem that needs intensive research in order to understand how and when it occurs. In this study electrochemical impedance measurements are performed on anodized aluminium panels. By anodizing aluminium its corrosion resistance is

improved. This improvement is to a large extent due to the increase in thickness of the barrier layer.

## Model anodized aluminium

When aluminium is anodized in sulfuric acid a porous and a barrier oxide layer are formed, while in tartaric acid only a barrier layer will be formed. The presence of a porous layer in sulfuric acid anodized aluminium can be attributed to the solubility of the oxide in sulfuric acid.

### The barrier layer thickness $d_b$

The thickness of the barrier layer depends linearly on the anodizing voltage  $E$ ; the proportionality factor  $r_a$  lies in the range of 1.0-1.4 nm/V. The thickness of the porous layer however depends on the anodizing time and the current density. The barrier layer thickness can be calculated using

$$d_b = (\epsilon_r \epsilon_0 A) / C_b$$

where  $\epsilon_r$  is the dielectric constant of the oxide layer,  $\epsilon_0$  the permittivity of vacuum,  $A$  the surface area of the working electrode and  $C_b$  the barrier layer capacitance.

## Results and conclusions

The electrochemical behavior of aluminium oxide is represented by the following equivalent circuit:

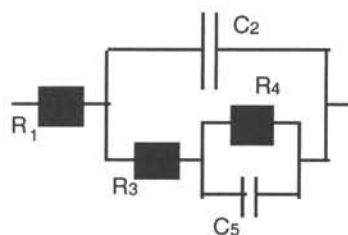
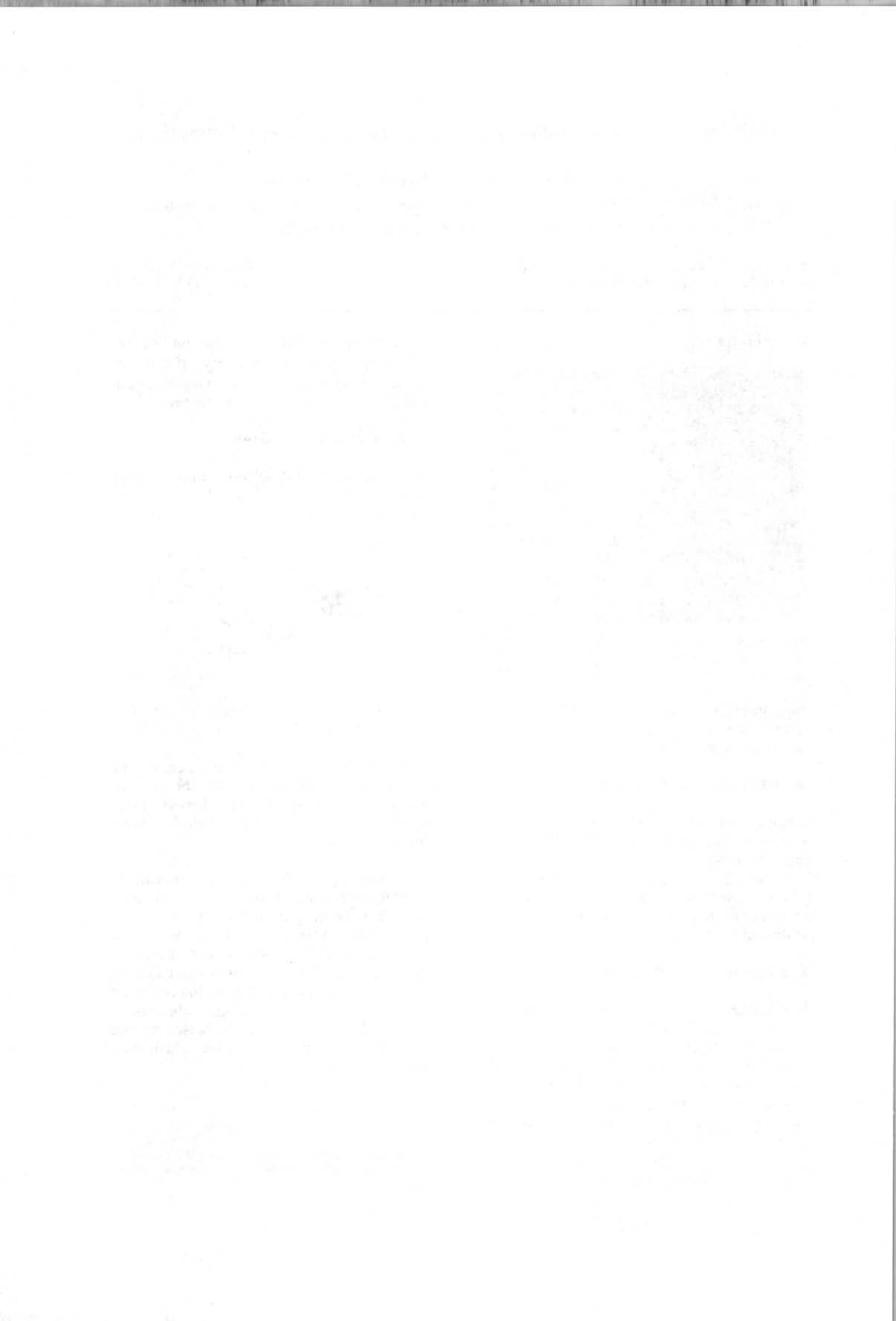


**Fig. 2:** Electrical equivalent circuit of the aluminium oxide layer

$R_1$  represents the solution resistance,  $C_2$  the double layer capacitance,  $R_3$  the charge transfer resistance,  $R_4$  the barrier layer resistance and  $C_5$  the barrier layer capacitance.

From the calculated values of  $d_b$  it can be concluded that the barrier layer thickness depends only on the anodizing voltage  $E$ . The proportionality factor  $r_a$  is nearly independent of the anodizing conditions but its value of 0.53 nm/V does not correspond with literature values. This deviation could be the result of a non linear relationship between  $E$  and  $d_b$  or could be caused by the dielectric constant of the oxide which may vary with thickness.

The Twente University of Technology (Dr.ir.V.J.Gadgil) and TNO Industry Delft (M.Hoeftlaak) are participants in this project.



# Heat Treatment Science and Technology

Groupleader: Prof.dr.ir. S. van der Zwaag  
Addres: Delft University of Technology  
Faculty of Chemical Technology and Materials  
Science  
Rotterdamseweg 137  
NL 2628 AL Delft  
+31-15-278 2248  
S.vanderZwaag @ STM.TUdelft.NL  
+31-15-278 6730



fax:

How to use the book

1. The first part of the book is a general introduction to the subject of the book. It is written in a simple and straightforward manner, and is intended to be read by all who are interested in the subject.

# The effect of inhomogeneous nitriding on the fatigue strength of the nitriding steel En40B

J.J. Braam, B. Pennings and S. van der Zwaag  
Heat Treatment Science and Technology,  
Laboratory for Materials Science,  
Delft University of Technology

Sponsor: FOM/TU Delft

Tel.: +31-15-2782197

E-mail: J.J.Braam@stm.tudelft.nl

B.Pennings@stm.tudelft.nl

**Introduction:** The phenomenon of non-nitridable surfaces is a common problem in industrial nitriding. In this research non-nitridable surfaces were prepared in a reproducible way and the effect of such non-nitridable spots on the fatigue strength of En40B was studied.

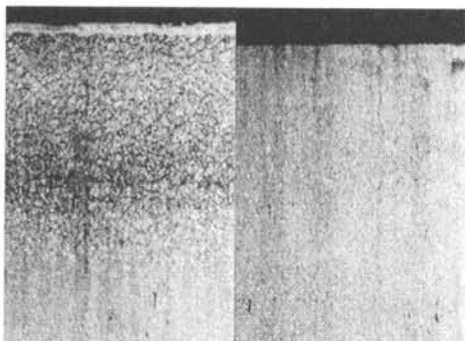


Figure 1: Nitridable (left) and non-nitridable En40B.

**Experimental:** Droplets of a sodium-metasilicate solution, an additive in machining/cleaning, were put in the notch of En40B steel fatigue testing specimens. After drying and nitriding this resulted in a complete absence of the diffusion zone and the compound layer (Fig.1). The specimens, having different spot diameters, were fatigue tested at several stress levels. Furthermore, finite element calculations were performed based on the model of local fatigue strength. The mesh and geometry are shown in Figure 2.

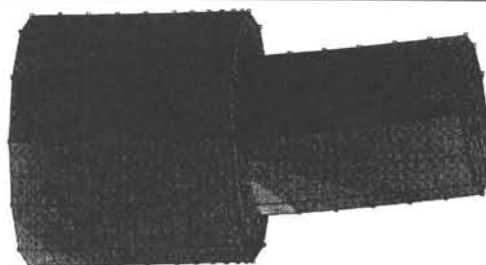


Figure 2: Mesh and geometry

**Results:** Figure 3 shows the results of the experiments and the calculations. Up to 3-4 mm, the fatigue limit decreases with increasing spot size. When the spots are larger than 4 mm (radius specimen: 7.5 mm) the fatigue limit after nitriding is not improved with respect to unnitrided specimens.

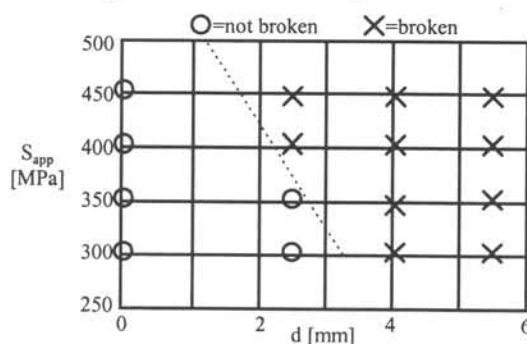


Figure 3: Fatigue strength vs. size of non-nitridable spot.

**Conclusions:** Small non-nitridable spots have a large influence on the fatigue limit of En40B. The calculations are in agreement with the experimental results.



# Filiform corrosion on coated aluminium alloys: the role of microstructural inhomogeneities in the substrate

Arjan Mol, D.C.M. Wilms, J.H.W. de Wit and S. van der Zwaag

Heat Treatment Science and Technology Group  
Corrosion Technology and Electrochemistry Group  
Laboratory for Materials Science

Sponsor: IOP Surface Technology

Tel.: +31 15 2785194

E-mail: J.M.C.Mol@stm.tudelft.nl

## Introduction

Filiform corrosion is a major point of concern when coated aluminium, iron or magnesium based alloys are exposed to a humid atmosphere. Most often this type of localised corrosion starts at defects in the coating such as cutting edges or local weak spots in the coating and is characterised by thread-like tracks. Filiform corrosion has been responsible for extensive damage, with extreme costs in various sectors of industry, such as building, automotive and aircraft. This type of localised corrosion is initially a cosmetic type of attack but depending on the application area of the alloy, it may result in more serious damage to the construction when left unattended.

Although several parameters influencing filiform corrosion behaviour have been discussed in the literature, the exact mechanism of filiform corrosion is still subject of discussion.

The aim of the present investigation is the determination of the effect of the microstructure, in particular its composition and its morphology, of aluminium based substrate materials on filiform corrosion.

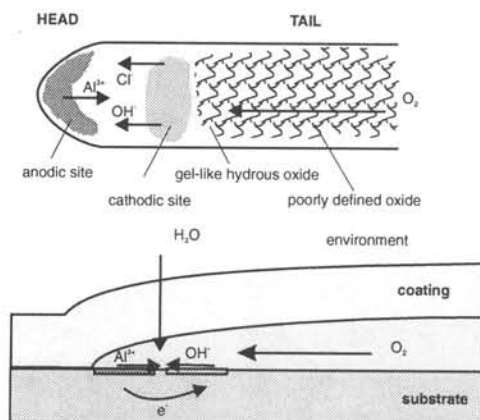


Figure 1: Cross-sections of the anodic undermining mechanism on aluminium substrates

## Mechanism of filiform corrosion

Filiform corrosion starts with the formation and growth of blisters. The factors influencing the initiation of blisters are also important for the initiation of filiform corrosion. The blisters may subsequently grow into uni-directional filaments. The factors which govern this transition are still unknown.

The propagation of filiform corrosion on aluminium substrates occurs according to the anodic undermining mechanism (Figure 1). The oxygen supply to the active head takes place through the tail of the filament in case of anodic undermining. This diffusion process is rather fast and as a consequence the propagation rate is determined by the rate of the anodic reaction in the head of the filament. Experimental results clearly show that the propagation rate depends on the corrosion properties of the alloy.

Very important for the present investigation is the fact that the initiation of blisters and the general corrosion properties of the aluminium alloy are closely related. The initiation of corrosion on (uncoated) aluminium alloys may start at local irregularities of the thin naturally present oxide layer on aluminium. These irregularities are related to the presence of elements like Cu, Mg and Si in solid solution or as intermetallic phases in the alloy. These local differences in composition influence the quality of the oxide layer over these phases, and as a consequence the protective properties. In particular, when copper-rich phases are present, the cathodic reaction preferably occurs at these particles which may lead to local corrosion phenomena.

## Project Overview

Generally, the influence of alloying elements can be investigated by determining the filiform corrosion properties of technical aluminium alloys, using a statistical analysis of the results. A disadvantage of this conventional procedure is the fact that it is impossible to characterise the initial local microstructure of the substrate after filiform corrosion attack. To obtain a clear insight into the mechanism of filiform corrosion and the substrate effects on a microstructural level, it is absolutely necessary to analyse the filiform corrosion properties of reproducible model substrates (figure 2), containing synthetic defects, which is the aim of the present investigation.

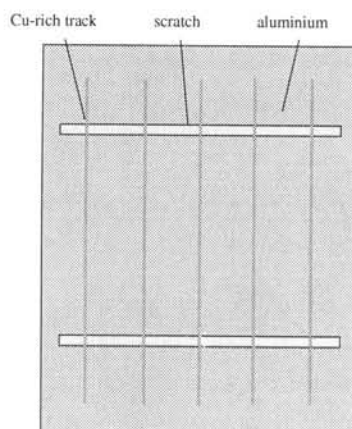


Figure 2: Schematic representation of coated Al/Cu model substrates, used for accelerated exposure tests



Figure 3: Example of cross-section of a diffusion zone of a Cu-rich track of an Al/Cu model substrate used for accelerated exposure tests

## Experimental

During the present investigation, filiform corrosion properties of model substrates are investigated on a laboratory scale by accelerated exposure tests. Corrosion experiments are performed on commercially pure aluminium sheet containing synthetic defects. These defects are generated by sputtering and consecutive diffusion treatment. A strict manufacturing procedure is inevitable to obtain reproducible model substrates.

The present set of experiments involve Al/Cu model substrates, as illustrated in Figure 2.

Copper-tracks are magnetron sputtered on commercially pure and chemically polished aluminium. Diffusion of copper into the base aluminium substrate is initiated by heat treating the specimens (Figure 3). Different sputter layer thicknesses and heat treatments are applied to compare different compositions and temper conditions. For the present set of experiments no industrial pretreatment is applied and substrates are only solvent cleaned with ethanol prior to coating.

After an organic coating is applied, line defects are scribed perpendicular to the copper direction, filiform corrosion is initiated by HCl-vapour and the specimens are exposed in a humidity cabinet at 40 °C and 82 % RH, according to DIN65472.

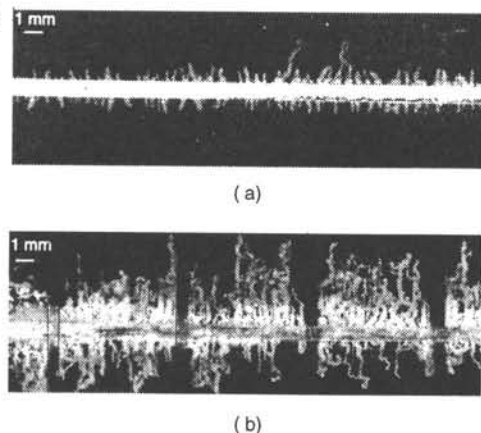
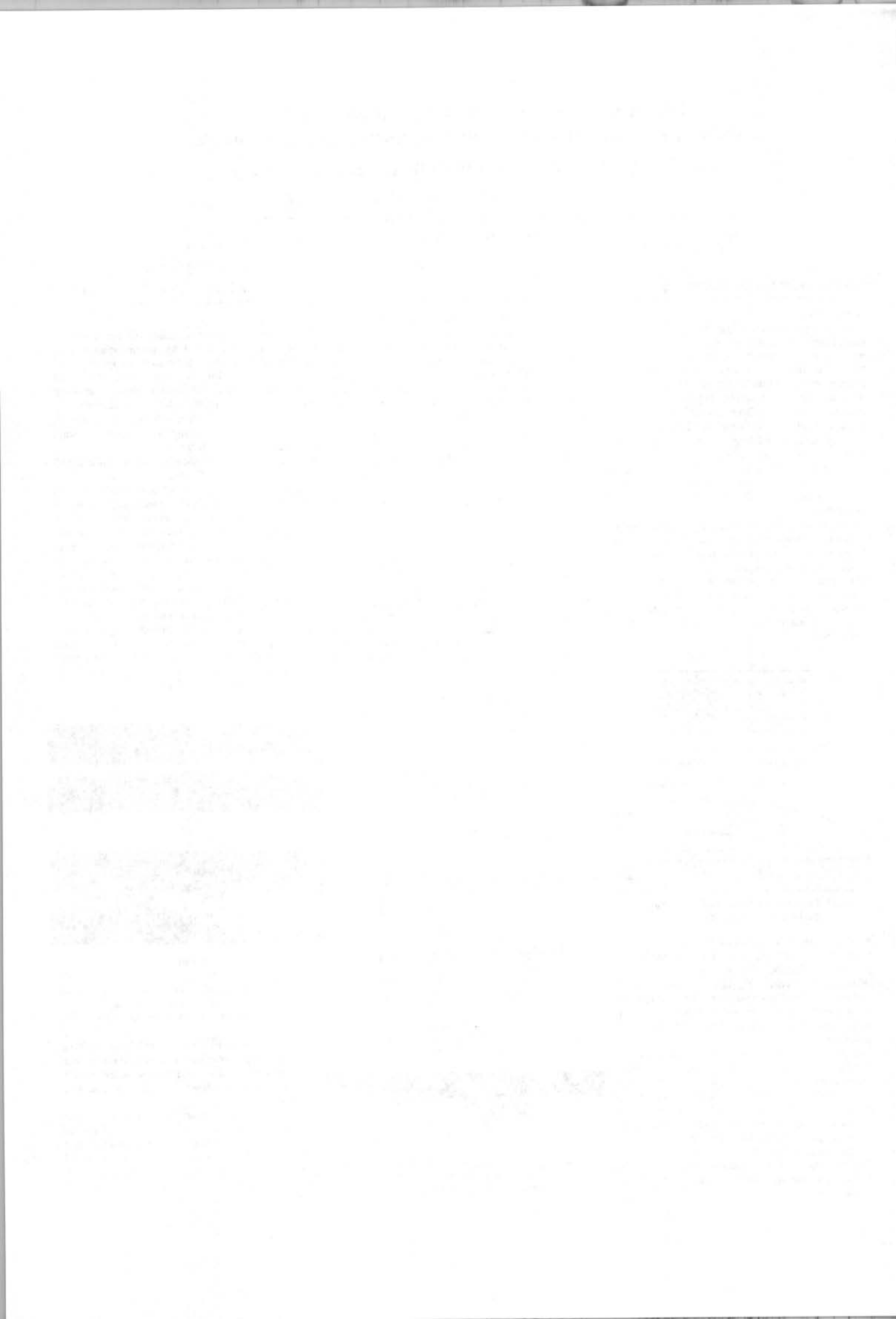


Figure 4: Filiform corrosion patterns on reference aluminium substrates (a) and Al/Cu model substrates (b) after 45 days of exposure according to DIN65472

Current observations show that mainly the filiform corrosion propagation is enhanced by the presence of Cu-rich artificial line defects and initiation and propagation is confined to the intermediate regions.

Besides further evaluation, future research of the investigation into the microstructural effects on filiform corrosion behaviour of aluminium based substrates will include the appliance of industrial pretreatments and coatings as well as local electrochemical measurements during filiform corrosion initiation and propagation.





# Advanced Materials and Casting Technology

Groupleader: Prof.ir. L. Katgerman  
Addres: Delft University of Technology  
Faculty of Chemical Technology and Materials  
Science  
Rotterdamseweg 137  
NL 2628 AL Delft  
+31-15-278 2249  
L.Katgerman@STM.TUdelft.NL  
+31-15-278 6730



fax:

# THE HISTORY OF THE CITY OF BOSTON

BY  
JOHN H. COLEMAN  
OF THE  
CITY OF BOSTON  
PUBLISHED BY  
J. B. LEECH, 15 NASSAU ST.  
N. Y.

# Metallurgical control of filiform corrosion of aluminium rolled products (FICARP)

*M.H.M. Huisert, D.H. van der Weijde, J.H.W. de Wit and L. Katgerman*

Sections Advanced Materials and Casting Technology and Corrosion Technology,  
Electrochemistry and Spectroscopy

This project is funded by the Brite/Euram programme

Tel.: +31-15-2785194

E-mail: M.H.M.Huisert@stm.TUdelft.nl

## Introduction

Filiform corrosion is a type of corrosion that can be found on coated aluminium, steel and magnesium. Filiform corrosion causes threadlike corrosion traces between the surface of the aluminium and the coating. The corrosion principle for the filiform is equivalent to a differential aeration cell. Oxygen is supplied through the tail of the filiform. Therefore the oxygen concentration decreases towards the head.

The key need in this project is to understand how the metallurgy of the aluminium substrate as determined by metal source, alloy composition, casting technique, processing and surface treatment influences filiform corrosion behaviour. The different aluminium substrates are characterised using electrochemical techniques, because this type of attack has an electrochemical origin. The first electrochemical techniques which are used are the measurements of the Open Corrosion Potential (OCP) versus time and polarisation curves.

## Electrochemical characterisation

Before the OCP is measured as a function of time, aluminium sheet material is degreased with ethanol. The OCP and polarisation curves are recorded with an Schlumberger SI 1286 ECI. This is done in an Avesta cell to prevent crevice corrosion on the aluminium.

Two examples of OCP measurements can be seen in figure 1. The OCP is recorded in two different electrolytes. These are a 5% NaCl acidic solution and a 0,5 % NaCl

neutral solution. The polarisation curves can be seen in figure 2.

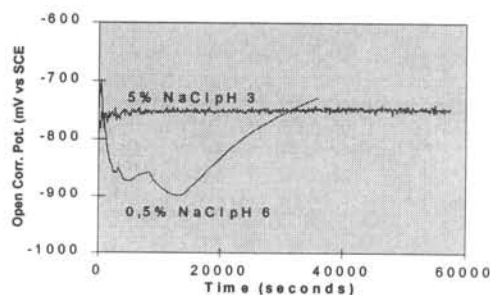


Figure 1. OCP measurement of AA 3005 versus time in different electrolytes.

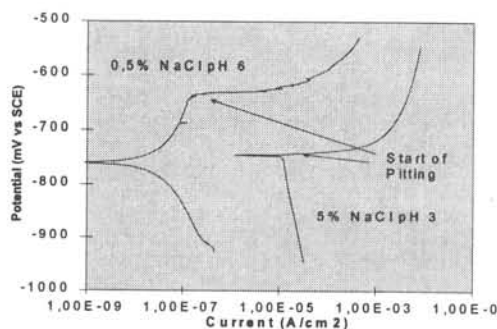


Figure 2. Polarisation curves of AA 3005 in different electrolytes.

In a 5% NaCl pH 3 solution the OCP stabilises much faster. This stable point is roughly at the pitting potential (see fig. 2). In a 0,5% NaCl solution the OCP decreases first to more cathodic potentials, then the OCP stabilises to almost the same potential as the 5% NaCl solution. This OCP is still below the pitting potential (see fig. 2). One can conclude that the corrosion current is about 100 times smaller in the neutral 0,5% NaCl solution than in the acidic 5% NaCl solution.

There is still a lot that can be done to fully understand the corrosion mechanism of filiform corrosion on aluminium.

THE UNIVERSITY OF CHICAGO

DEPARTMENT OF THE HISTORY OF ARTS

AND ARCHITECTURE

OFFICE OF THE DEAN

540 EAST 58TH STREET

CHICAGO, ILLINOIS 60637

TEL: 773-936-5000

FAX: 773-936-5001

WWW.HA.UCHICAGO.EDU

ADMISSIONS

1. APPLICATIONS

2. ADMISSIONS

3. FINANCIAL AID

4. STUDENT LIFE

5. CONTACT US

6. ABOUT US

7. FAQ

8. CAMPUS TOUR

9. STUDENT ORGANIZATIONS

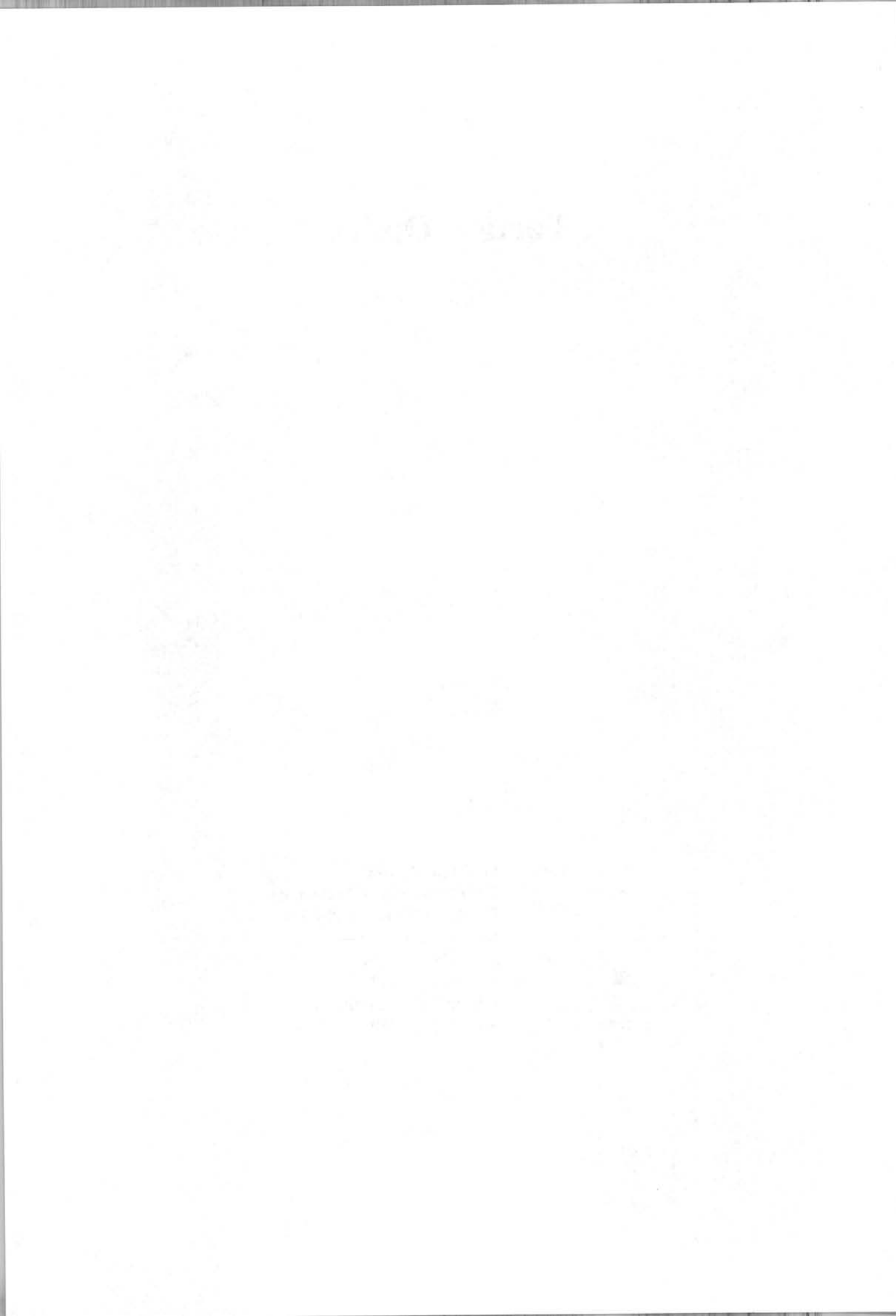
10. ALUMNI

# Particle Optics

Group leader: Prof.dr.ir. P. Kruit  
Address: Delft University of Technology  
Faculty of Technical Physics  
Lorenzweg 1  
NL 2628 CJ Delft  
+31-15-278 5197  
P.Kruit@TN.TU Delft.NL  
+31-15-278 3760



fax:



# A parallel detector for Auger spectroscopy in an electron microscope

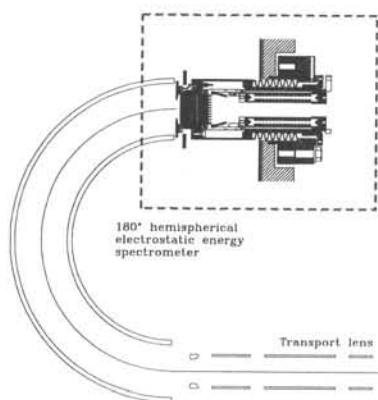
J.S. Faber<sup>1</sup>, C. Smit and P. Kruit

Delft University of Technology, Department of Applied Physics, Lorentzweg 1, 2628 CJ Delft

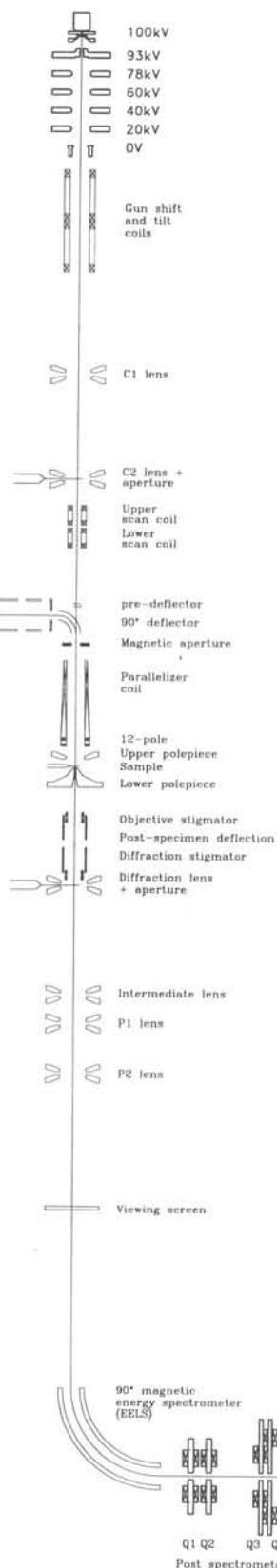
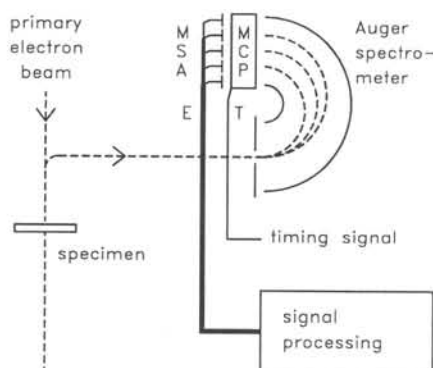
<sup>1</sup> Present address: Philips Electron Optics, P.O. Box 218, NL-5600 MD Eindhoven

## Introduction.

A Philips EM430 transmission electron microscope has been adapted to allow detection of both Auger and energy loss electrons. This opens the way for



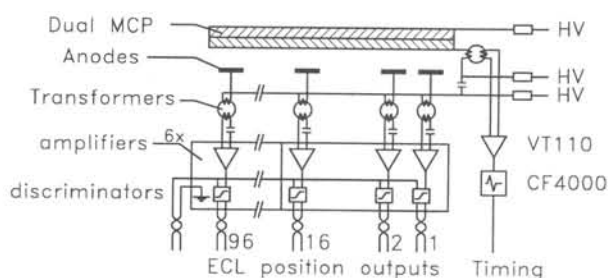
nanometer resolution elemental mapping of surfaces and for coincidence spectroscopy. To overcome the low count rates normally associated with coincidence experiments we are developing a parallel detector for the Auger spectrometer.



## Auger spectrometer

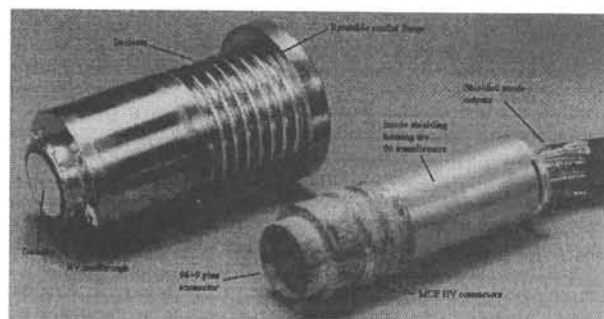
Primary electrons from the gun excite the specimen. This results in the emission of Auger electrons which are directed upwards along the optical axis by the magnetic field of the objective lens and the parallelizer. The 90° deflector bends the Auger electrons towards the hemispherical analyzer. The settings of the transport lens and the analyzer determine the energy range and resolution on the strip anodes of the parallel detector.

## Parallel detector design

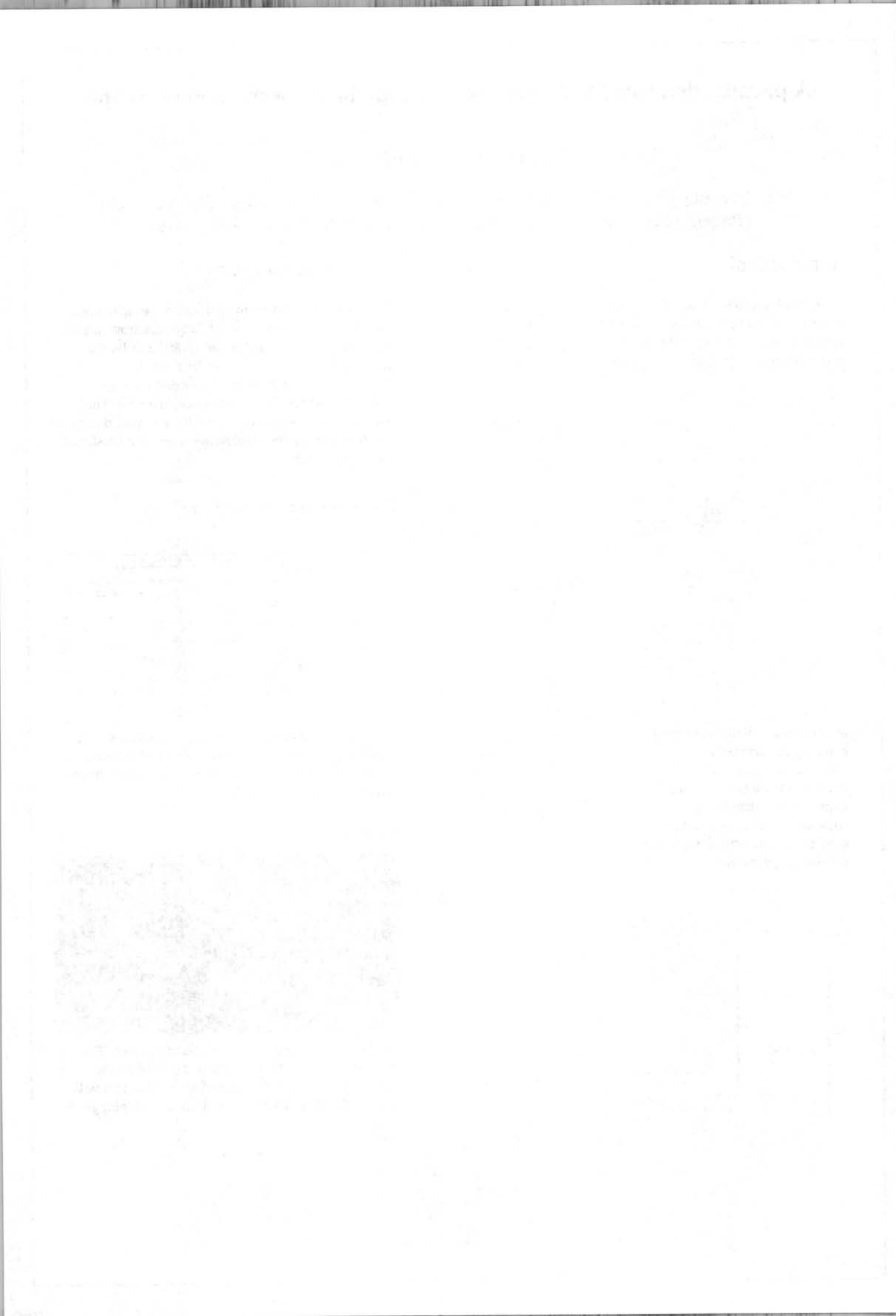


The Auger detector is a completely parallel detector, consisting of a multi channel plate (MCP) followed by a multi strip anode. Each anode is connected to its own preamplifier and discriminator

## Result



This is the unmounted detector. Normally a MCP is situated in front of the detector with the 96 anode strips. The connector has 96 spring contacts that will connect the strips with the electronics when plugged in.





# DIMES / NanoPhysics and - Technology

Substitute Groupleader:

Address:



fax:

Dr. G.C.A.M. Janssen

Delft University of Technology

Faculty of Technical Physics

Lorenzweg 1

NL 2628 CJ Delft

+31-15-278 6297

G.C.A.M.Janssen@DIMES.TUdelft.NL

+31-15-278 8820



# Nanoscale Structures Composed by Selective Thermal CVD and STM Stimulated Decomposition of Dimethylaluminumhydride

*E. Boellaard and G.C.A.M. Janssen*

*Department of Applied Physics, DIMES/S NEXT-lab*

Sponsor: FOM / TU Delft

Tel: +31-15-2782494

E-mail: boel@dimes.tudelft.nl

## **Introduction**

In the NEXT-project we will study the physical properties of molecular and metallic structures of very well controlled shape and high purity in a size regime where the quantization of the energy of the electrons is important. The development of the technology for the fabrication of very small metallic aluminum structures is the subject of this specific part of the project.

## **Recent**

It has been demonstrated that aluminum can be selectively deposited onto silicon. This means that aluminum is deposited on silicon and not on silicon dioxide which is used to mask the silicon substrate. Aluminum deposited from dimethyl aluminum hydride (DMAH) is in addition deposited epitaxially onto silicon. By a careful choice of the silicon surface orientation one can prescribe the orientation of the aluminum. The crystals grown so far are in the 1  $\mu\text{m}$  range. We will use the same chemistry but improve on the lithography to arrive at patterns in the nanometer range.

The chemical vapour deposition (CVD) experiments with DMAH will be performed in an ultra high vacuum (UHV) system in order to stabilize the small metallic structures. Over the past two years a large multichamber UHV system has been build which provides facilities for *in situ* substrate cleaning, structure preparation and manipulation on atomic scale, characterisation and measurements.

## **Present**

In order to reduce the dimensions of the deposited aluminum structures, silicon with a 10 nm silicon dioxide toplayer will be covered with a standard resist after

which a pattern will be written by the Electron Beam Pattern Generator (EBPG) at DIMES. After development the pattern will be transferred into the oxide by means of plasma-etching. On the thus prepared substrate aluminum will be deposited selectively. The typical resolution of this process is limited to about 20 nm.

## **Future**

The dimensions of the deposited aluminum structures can be further reduced by using resists which permit higher resolutions: e.g. atomic hydrogen. After dipping a silicon wafer in dilute fluoric acid the surface is hydrogen terminated. This surface can be used as a negative resist. Areas irradiated by electrons lose their hydrogen termination. During the subsequent CVD process, aluminum will only be deposited on surface areas where the hydrogen termination is still intact. The ultimate resolution is limited by the diameter of the electron beam. Lithography by electrons from a scanning tunneling microscope (STM) has already demonstrated 5 nm resolution.

In an other approach aluminum structures will be directly written by STM. For several precursors it has been demonstrated that the adsorbed precursor molecules can be decomposed by electrons tunneling from the STM tip to the substrate. We expect that this will also be the case for DMAH.

The latter experiments will be performed with a new home-build STM, which is presently being developed.



# Temperature dependant morphology changes of CoSi<sub>2</sub> thin films

*B. Ilge, G. Palasantzas, J.M.M. de Nijs, L.J. Geerligs,*

*Department of applied Physics , NEXT lab.*

sponsor : FOM / TU Delft

tel.: +31 15 278 7163  
e-mail: ilge@cerberus.dimes.tudelft.nl

## Introduction

CoSi<sub>2</sub> forms atomically flat surfaces and interfaces with the Si (111) substrates. This makes it an ideal candidate for well defined mesoscopic structures and leads compatible with STM Lithography (STM = scanning tunneling microscope). Therefore the formation and the thermal stability of such structures under UHV conditions is of growing interest.

## Experiment

0.5 nm Co is evaporated on the clean 7x7 reconstructed Si surface. The change of surface morphology after different heat treatments is monitored with in situ STM.

## Results

After room temperature deposition the surface of the pure substrate is just altered by an additional surface corrugation of a few Å (Fig.1) . After annealing at 600° C all the Co has been consumed in the silicidation process and the whole surface is covered by the disilicide film (Fig.2). This film morphology changes drastically after an additional heat treatment at ca. 900° C (Fig.3). Between the CoSi<sub>2</sub> islands of upto 12 nm high the bare Si becomes visible. A further short annealing at 1200° leads to a disappearance of the silicide islands and the surface changes to a morphology similar to the clean Si substrate where the 7x7 reconstruction is replaced by the Co induced  $\sqrt{7}\times\sqrt{7}$  reconstruction (Fig.4).

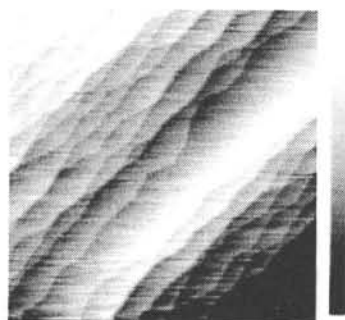


**Fig.1**

surface after deposition ; size 800 nm ; gray scale 1.3 nm

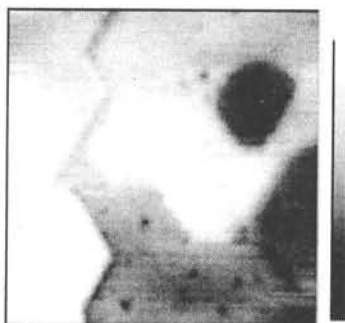


**Fig.2**

disilicide film ; size: 62 nm ; gray scale 0.34 nm

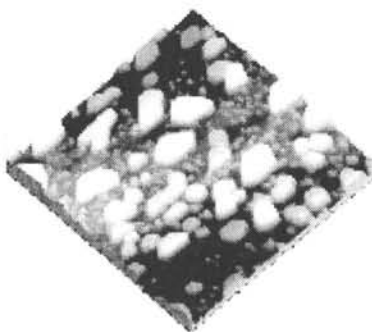


**Fig.3**

surface after island formation ; size: 2000 nm ; gray scale 10 nm

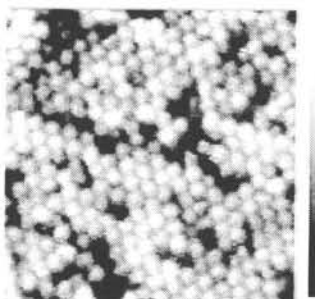


**Fig.4**

Co induced reconstruction ; size: 16 nm; gray scale 0.19 nm



# High Pressure Extrusion of Aluminium for Sub-micron Vias

J.F. Jongste, J.P. Lokker, G.C.A.M. Janssen and S. Radelaar

DIMES, Nano Physics and Technology, Delft University of Technology

Sponsor: FOM, EU

tel: +31 152782600

e-mail: jongste@dimes.tudelft.nl

## Introduction

In 1994 a new method has been introduced to form high aspect ratio ULSI sub-micron diameter Al vias with high quality.<sup>1</sup> As an alternative to eliminate the poor step-coverage of a conventional metallization process (sputter-deposition), high pressure extrusion ("force-fill") of aluminium provides improved via-fill. The method can be described as the extrusion of a bridging Al layer into a via opening using high pressure thus providing a connection to the lower level in the circuit. The process runs at elevated temperature, driven by hydrostatic pressure (typically 400°C and 60 MPa). At DIMES this process is explored with silicone oil (polymethyl-siloxane) as pressure transducer. The mechanism and kinetics of the process are still unclear. The relation between pressure, temperature and filling rate of the process is investigated.

## Results

Al-Cu (0.5%) films (800 nm) have been sputter-deposited on patterned oxidised wafers [covered by TiN (100 nm)]. Fig. 1 shows cross-section SEM images of vias as deposited (a) and *force-filled* at 280°C, 80 MPa, 16 min. (b).

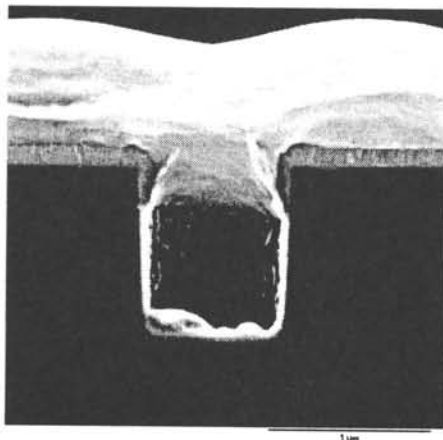


Fig. 1 a. SEM image of Al via (as dep.).

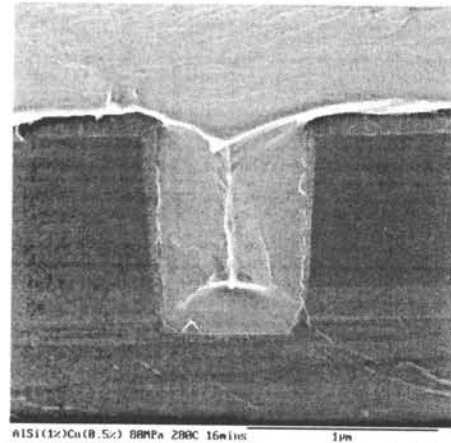


Fig. 1b. SEM image of force-filled Al via.

Fig. 2 shows the relation between pressure, temperature and via-fill. From Fig. 2 it is found that a threshold stress exists below which no plastic deformation takes place (50 MPa). In Fig. 2 a strong dependence on pressure and temperature is shown. At present, the process is being characterized by means of kinetic analysis. As yet, the results as shown here are described in a model of a stress-driven diffusion process.

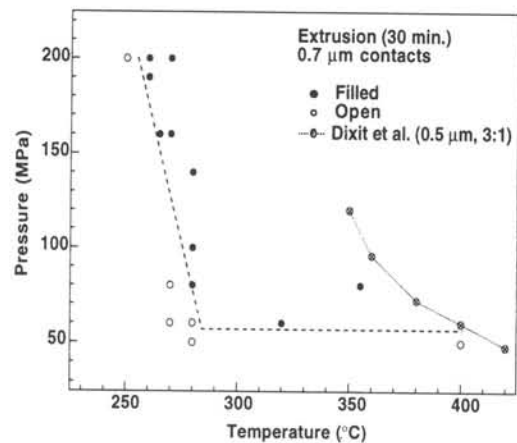


Fig. 2. Relation between pressure, temperature and filling capability.

<sup>1</sup> Dixit G.A., M.F. Chisholm, M.K. Jain, L.M. Ting, S. Poarch, K. Mizobuchi, R.H. Havemann, Proceedings of IEDM 1994, p 105 - 108.

1870

1871

1872

1873

1874

1875

1876

1877

1878

1879

1880

1881

1882

1883



# Origin of resistance changes due to electromigration in Al lines

A.H. Verbruggen, M.J.C. van den Homberg, L.C. Jacobs and S. Radelaar

Delft Institute of Microelectronics and Submicron Technology, Delft University of Technology

Sponsor: TUD/FOM

Tel.: + 31 - 15-2786124

E-mail: ahv@dimes.tudelft.nl

High-resolution resistance measurements have been used to study fundamental aspects of electromigration in thin film pure Al conductors. The sample layout is shown in Fig.1. Passing a DC through one of the lines changes the resistance of the line due to electromigration. The other line serves as a reference. The lines are 2  $\mu\text{m}$  wide and 110-115 nm thick. The measurements were carried out between 150  $^{\circ}\text{C}$  and 200  $^{\circ}\text{C}$ .

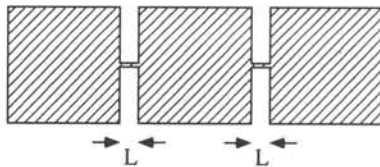


**Fig.1.** Sample layout for AC bridge resistance measurements ( $3 \leq L \leq 17 \mu\text{m}$ ).

An example of a measurement is shown in Fig.2. After a period of 20 to 60 minutes the DC stressing current is switched on and an immediate increase of the resistance is observed corresponding to Joule heating. This is followed by an increase of the resistance. Depending on DC current density and sample length the resistance saturates (Fig.2A) or increases linearly with time (Fig.2B). When the current is switched off after a few hours we see, following the immediate effect of removing the Joule heating, a complete relaxation of the resistance to its original value (Fig.2A) or only a partial recovery (Fig.2B). Fig.3 is an AFM micrograph of a line that displayed a permanent resistance change. From many detailed studies we conclude that the recoverable resistance changes are due to the build-up of mechanical stress and the non-recoverable changes to the formation of a void or hillock.

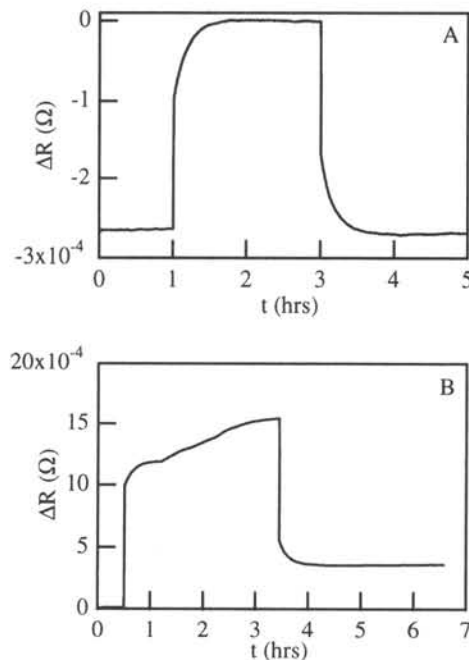


**Fig.2.** Resistance changes induced by electromigration as function of time. A:  $j = -2 \text{ MA/cm}^2$ , B:  $j = -4 \text{ MA/cm}^2$ .  $L = 8 \mu\text{m}$ ;  $T = 150^{\circ}\text{C}$ .

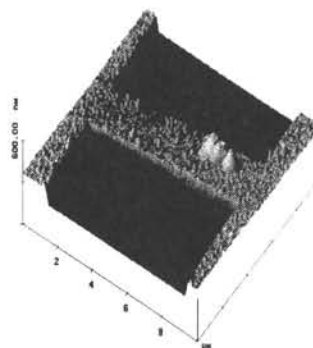


**Fig.3.** AFM picture of a sample after stressing at  $j = 3 \text{ MA/cm}^2$  at  $150^{\circ}\text{C}$  for 6 hours.

## References

A.H.Verbruggen et al., Materials Reliability in Microelectronics VII, Mat. Res. Soc. Symp. Proc. 473 (1997)



# Radiation Physics

Groupleader: Prof.dr.ir. L.A. de Graaf  
Addres: Delft University of Technology  
Interfaculty Reactor Institute  
Mekelweg 15  
NL 2629 JB Delft  
+31-15-278 5545  
L.A.deGraaf@IRI.TUdelft.NL  
+31-15-278 6422



fax:



# Production and Characterisation of Polyelectrolyte Multilayers

R. Bijlsma, A.A. van Well

Afdeling Stralingsfysica, Interfacutair Reactor Instituut

Sponsor: NWO/SON

Tel: + 31-15-2787109

E-mail: Rita@iri.tudelft.nl

## Introduction

In last decade, the interest in thin organic films is increasing strongly. Applications are found in a variety of research areas, such as integrated optics, sensors, organic solar cells, drug delivery and friction reducing coatings. In collaboration with the University of Wageningen, we developed a new self-assembly technique to produce organic multilayer systems, that may provide the desired control on the architecture at the molecular level. The multilayers are produced by alternately immersing a charged substrate (e.g. silicon or glass) into aqueous solutions of oppositely charged polyelectrolytes (see Fig.1).

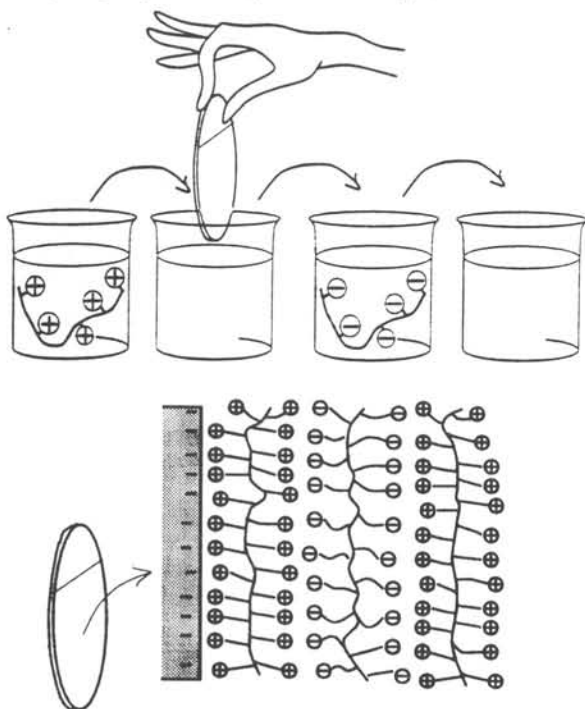


Fig.1 Self assembly of the multilayers

The aim of our study is to characterise the structure of these films, and to determine and understand the relation between this structure and the growth conditions (e.g. type, charge and size of polymers, concentration, ionic strength, pH).

## Experiment

We confirm the self-assembly process by in-situ determination of the adsorbed amounts, by optical reflectometry. Using neutron reflectometry (NR), we determine the internal structure of the film. This technique yields the neutron refraction index depth profile, in the range from 1 to 300 nm. In principle, we obtain from NR information about monolayer densities and thicknesses, total film thickness, and water contents. First experiments were done at the IRI reflectometer ROG. The polyelectrolytes we used were PVP<sup>+</sup> (poly(1-methyl-2-vinyl pyridine), M = 120k), and PSS<sup>-</sup> (poly(p-styrene sulphonate), M = 88k). The polymer concentrations were as low as 100 ppm by weight. The substrate was silicon. We made systems consisting of up to 40 bilayers.

## Results

The bilayer thickness depends on the ionic strength of the solutions during assembly, and of the water content of the film. For a dry sample, grown at a low ionic strength (5 mM), the bilayer thickness is 0.65 nm, i.e. the polymers lie flat on the surface. By doubling the ionic strength, the bilayer is a factor 1.6 thicker. The polymer density is approximately 1 g/cm<sup>3</sup>, in both cases. The film appears to be rather hygroscopic, it can absorb up to 42% of water, swelling accordingly.

## Future

We started to study the PVP-PSS stoichiometry, and the presence and amount of counterions built in, using NR and neutron activation analysis. Performing especially designed NR experiments, using deuterated polymers, will yield information of the interpenetration of the polymer layers. Furthermore, we will model the conformation of the polymers using self-consistent field calculations.

Subscription price, Five Dollars per Annum in Advance. Single Copies, Fifteen Cents.  
Entered as Second-Class Matter, May 2, 1882. Postpaid at Special Rate of \$3.75 per Annum.  
Acceptance for mailing at Special Rate of \$3.75 per Annum authorized March 3, 1917.  
Postmaster: This publication is paid for at the rate of \$3.75 per annum.  
Copyright, 1919, by American Medical Association

**Editorial**  
In the past few years, the medical profession has been subjected to a series of attacks from the public and the press. These attacks have been based upon a number of false premises and have been the result of a general ignorance of the facts of the situation. The medical profession is a noble one, and its members are devoted to the service of their fellow men. They are not interested in money or power, but in the health and happiness of the community. The attacks upon the profession have been the result of a number of factors, including the increasing cost of medical care, the complexity of modern medicine, and the general ignorance of the public. It is the duty of the medical profession to educate the public and to defend itself against these attacks. This journal is one of the many ways in which the profession can do this. It is a forum for the discussion of medical problems and for the expression of the views of the profession. It is a place where the facts can be set forth and where the public can be educated. We hope that this journal will continue to be a valuable service to the medical profession and to the public.

**Original Article**  
The following article is a contribution to the knowledge of the medical profession. It is a study of the effects of certain drugs upon the human body. The author is a member of the medical profession and is qualified to write on this subject. The article is a valuable contribution to the literature of medicine and is one of the many ways in which the medical profession can advance its knowledge. The article is a study of the effects of certain drugs upon the human body. The author is a member of the medical profession and is qualified to write on this subject. The article is a valuable contribution to the literature of medicine and is one of the many ways in which the medical profession can advance its knowledge.

**Book Reviews**  
The following are reviews of books recently published. These reviews are written by members of the medical profession and are one of the many ways in which the profession can keep abreast of the latest developments in medicine. The reviews are a valuable service to the medical profession and to the public. They are a way in which the profession can share its knowledge and can keep the public informed of the latest developments in medicine. The reviews are a valuable service to the medical profession and to the public. They are a way in which the profession can share its knowledge and can keep the public informed of the latest developments in medicine.